Journal of Polymers and the Environment (2023) 31:4662–4690
https://doi.org/10.1007/s10924-023-02899-7

REVIEW

PLA, PBAT, Cellulose Nanocrystals (CNCs), and Their Blends: Biodegradation, Compatibilization, and Nanoparticle Interactions

Fernanda Andrade Tigre da Costa[1] · Duclerc Fernandes Parra[1] · Elizabeth Carvalho Leite Cardoso[1] · Olgun Güven[2]

Accepted: 24 April 2023 / Published online: 3 June 2023

Abstract

PLA/PBAT (Poly (lactic acid)/Poly (butylene adipate-co-terephthalate)) blend is a biodegradable material commonly considered a potential alternative to polymeric products from petroleum sources. PLA is intrinsically brittle, endowed with a low elongation at break and poor impact strength that restricts its use for some applications while PBAT has high ductility, heat resistance, and impact resistance. However, PLA associated with PBAT results in an incompatible blend, due to poor interfacial adhesion. The compatibilization of PLA/PBAT can be improved through physical and chemical interaction between the components, and with exposure to ionizing radiation. Cellulose is the most abundant biodegradable polymer available and is considered the potential material to be used as reinforcement in sustainable composite materials, as well as nanocellulose while an alternative to synthetic nanoparticles. This review describes the state of the art of polymer blends of PBAT and PLA, in terms of manufacturability, compatibilization, biodegradation, radiation processing, and cellulose nanocrystal reinforcement.

Keywords PLA · PBAT · Blends · Nanocellulose · Compatibilization

Introduction

PLA or Poly(lactic acid) is a renewable, bio-based and biodegradable aliphatic thermoplastic polyester made from dextrose (sugar) extracted from biobased materials [1–6]. Biobased plastics come from renewable biomass, meaning plants. Some common plants that are used to make bioplastics are sugarcane, cassava, and corn. PLA is a popular biopolymer and currently produced on a worldwide scale. Biopolymers are polymers that are biobased, biodegradable, or both, and have the same properties as conventional polymers and offer additional advantages. In addition, PLA products exhibit good bio-absorption and biocompatibility with the human body, in favor of more potential applications [7]. However, PLA has low melt strength, which limits its application in large-scale blown film extrusion processes. Meanwhile, PBAT is one of the most attractive polymers for hardening PLA [8].

PBAT (polybutylene adipate terephthalate) is a fully biodegradable polymer. Instead of PBAT-based compostable bioplastics will decompose due to the action of naturally occurring microorganisms such as fungi, algae and bacteria. Plastics that are based on fossil resources and are biodegradable, such as PBAT, despite being manufactured from petroleum-based resources, are fully biodegradable under composting conditions [9–16].

Considering complementary properties involving PLA and PBAT, the PLA/PBAT blends have been receiving special and wide attention all around the world [17–21]. And concerning the processability of blends, important aspects should be discussed in terms of the efficiency, manufacturability, and utility of those materials.

Several important aspects must be considered from the point of view of the design and manufacture of PLA/PBAT blends. The morphological, thermal, rheological, and mechanical properties must be controlled and optimized to contribute to the compatibilization and interface situation of the blend [22, 23]. The combination of PLA and PBAT provides immiscible blends, and the final properties of the blends are highly dependent on the intrinsic and

✉ Fernanda Andrade Tigre da Costa
fernanda.tigre@outlook.com

[1] Department of Chemistry and Environment, Nuclear and Energy Research Institute, IPEN, CNEN/SP, São Paulo - SP, Brazil

[2] Department of Chemistry, Hacettepe University, Ankara, Turkey

morphological properties of the PLA and PBAT, which can be significantly improved by chain extender and compatilizer [24].

Compatibilization is a process by which the polymer blend properties are enhanced owing to an increase of adhesion between the phases, as a result of the interfacial tension reduction and morphology stabilization. The degree of miscibility between the components in blends can be enhanced through the addition of compatibilizers [25].

During the last decade, cellulose nanocrystals (CNC) embedding has been widely investigated in polymer matrices such as PLA and PBAT due to their good optical properties, low density and natural abundance [26–31]. Cellulose nanocrystals are important for the final performance of polymer blends and can be improved by introducing nanoparticles as reinforcements and simultaneously a compatibilizer [32, 33]. The localization of nano-inclusions at the interface, in the matrix, or dispersed phase has a significant effect on blend properties [34].

This review aims to present the latest results obtained in the literature on the properties of PLA, PBAT, crystalline nanocellulose and their blends in terms of compatibilization, biodegradation and nanoparticles interactions in the properties of this biodegradable blend.

Poly(lactic acid)—PLA

Poly(lactic acid) (PLA) is considered one of the most competitive biodegradable polymers due to its advantages of good mechanical strength, biocompatibility and as a renewable raw material [35]. PLA has several forms of end-of-life applications related to its biodegradability, among them, it can be recycled mechanically or chemically, it can be industrially composted and also be digested anaerobically [36].

PLA is an organic, aliphatic, thermoplastic polyester consisting of a racemic mixture of D-lactide and L-lactide, having two optically isomeric forms: PLLA and PDLA, as shown in Fig. 1a. And it can be derived from corn starch and sugarcane [37, 38].

Due to its recyclable, biodegradable, and compostable properties, PLA is widely used in packaging, transportation, agriculture, biomedical, textile, and electronics industries [41]. Despite its great potential, PLA still has some limitations, such as fragility, slow crystallization kinetics, and high instability during processing, among others [42].

PLA Mechanical Properties

The mechanical properties of PLA can vary according to the molecular weight and degree of crystallinity, where lactide monomers are chiral and the mechanical properties can be manipulated through the polymerization of D-lactide,

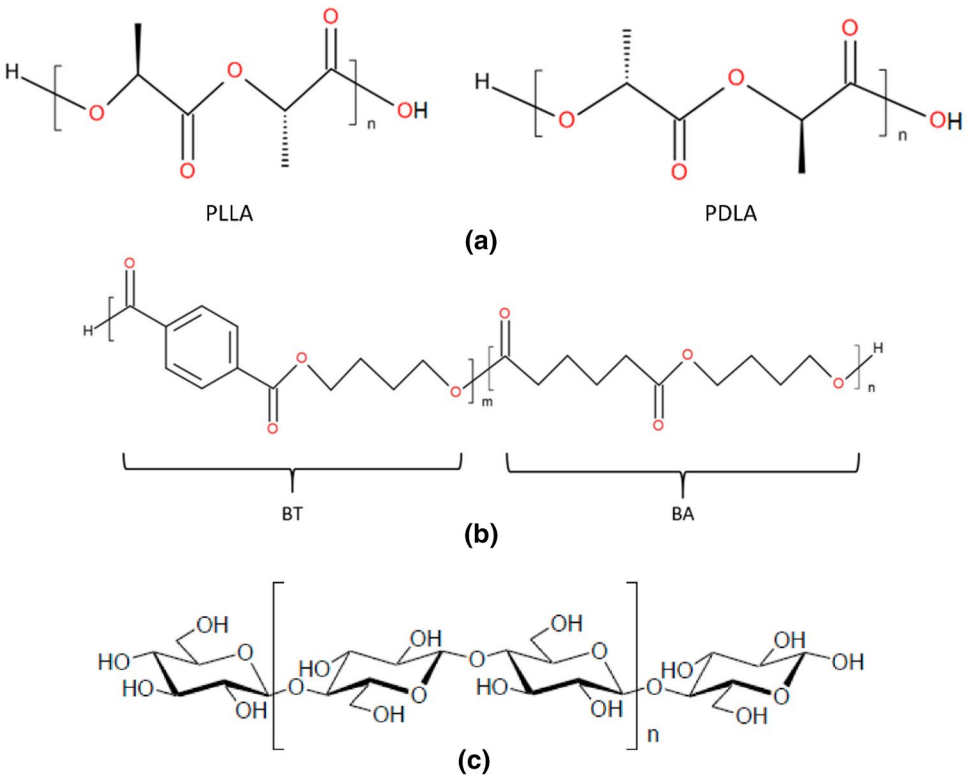

Fig. 1 Chemical structure: **a** of PLA isomers: PLLA and PDLA; **b** of PBAT; **c** of cellulose Reproduced with permission from MDPI [38–40]

L-lactide or D, L-lactide to obtain the desired properties [43]. Some of these properties are shown in Table 1.

Commercial PLAs are generally copolymers of PLLA and PDLLA. L-lactic acid rotates the plane of polarized light clockwise, unlike D-lactic acid, which rotates counterclockwise. Lactic acid produced from petroleum is a racemic mixture (50/50) of the D and L units, so it becomes optically inactive. The fermentation method (more ecological) transforms, for example, corn starch into lactic acid, in which the L-isomer is the main product of the natural PLAs in the fermentation process (99.5% of the L-isomer and 0.5% of the D-isomer) [44].

PLA Biodegradation Properties

Standard biodegradation tests for plastics in composting conditions, such as the ASTM D5338-98 [45]; consider plastic to be biodegradable, through the percentage of biodegradation concerning the positive reference (cellulose = 100%) in which sufficient biodegradation (minimum 70% for cellulose in 45 days) must be observed. And the standard biodegradation test for plastics in soil, such as ASTM D5988 [46]; considers a plastic to be biodegradable by referring to known biodegradable reference material (such as starch or cellulose) to verify soil activity. Where, after six months, limited biodegradation needs to be higher than 70% of the theoretical evolution of CO_2 for this reference material, and the amounts of carbon dioxide released from the blanks (or the biochemical oxygen demand values for the alternative measurement of oxygen consumption) must be within 20% of the mean at the plateau or at the end of the test.

The biodegradation of PLA is a two-step process, chemical hydrolysis or hydrolytic degradation followed by biodegradation. In the first step, the degradation of PLA occurs through random chain scission, which reduces the molar mass of chains and leads to the intermediate formation of low molecular weight chains. In the second step, these intermediate chains are assimilated by the microbes to obtain energy and produce various compounds such as CO_2 and H_2O [47]. Table 2 summarizes different types of PLA and their biodegradation results.

It is known that the degradation of PLA in the soil is slow and takes a long time to initiate degradation, probably because of the slow rate of hydrolysis at low temperatures, moisture contents, and the relative scarcity of PLA degrading organisms. But in a composting environment, the PLA is hydrolyzed into smaller molecules after 45–60 days at 50–60 °C [48]. In Table 2 it is possible to observe that PLA has high biodegradation according to the studies in composting environments and can be fully biologically degraded within 6–24 months [49], which may vary according to the biodegradation conditions, such as pH, temperature and other factors.

Currently, several types of microorganisms that are capable of degrading PLA have been isolated from soil and water, which are mainly actinomycetes, a fraction of them belong to bacteria and fungi [50]. At least 94 microorganisms are cataloged as being able to degrade PLA (31 fungal and 63 bacterial species). This compatibility of PLA degradation by these microorganisms is also related in the literature by the similarity of the L-lactate unit of PLA with the L-alanine unit of silk fibroin (a fibrous protein produced by domestic silkworms that is a natural analog of poly(L-lactide)). Wherein, the bacterial genus *Amycolatopsis*, which had the highest number of reported PLA degraders, also has several reported species that degrade silk fibroin, possibly

Table 1 Physical and mechanical properties values of PLA, its isomers and PBAT

Properties	PLA poly(lactic acid)	PLLA poly(L-lactic acid)	PDLLA poly(D,L-lactic acid)	PBAT poly(butylene adipate co-terephthalate)	References
Density (g/cm^3)	1,21–1,25	1,24–1,30	1,25–1,27	1,23	[141, 142]
Melting temperature (ºC)	150–162	170–200	not defined (amorphous)	110–120	[24, 121, 142]
Glass transition temperature (ºC)	45–60	55–65	50–60	− 33–− 29	[24, 142, 143]
Crystallization temperature (°C)	108,3	80,44	101,47	73,9	[144–146]
Tensile strength (MPa)	21,0–60,0	15,5–150	27,6–50,0	11–21	[89, 142, 143, 145, 147]
Tensile modulus (GPa)	0,35–3,50	2,70–4,14	1,00–3,45	0,026–0,29	[89, 142, 147, 148]
Flexural strength (MPa)	89,4	106	88	6,3–7,3	[75, 146, 149]
Flexural modulus (MPa)	3098	3650	–	70–90	[75, 146, 150]
Elongation at break (%)	5,0	7	5,4	> 600	[89, 121, 145, 149]
Ultimate strain (%)	2,50–6,00	3,00–10,0	2,00–10,0	–	[142]

"- " Unknown

Table 2 Biodegradation of some forms of PLA, PBAT and PLA/PBAT blends reported in the literature

Type of polymer	Biodegradation conditions	Test method	Biodegradation time	pH conditions[a]	Temperature conditions[b] (°C)	Moisture conditions[c] (%)	Reference
PLA							
PLLA films (Natureworks, 4032D)	Under controlled composting conditions, method by analysis of evolved CO_2	GB/T 19,277–2003 ISO 14855–2005	78.9% of weight loss after 80 days	7,2	–	53,5	[151]
PLLA films (NatureWorks 4043D)	Under thermophilic anaerobic conditions	ISO 15985	60 ± 18% of weight loss after 75 days	7,14–7,73	52 ± 2	–	[152]
PLLA films (NatureWorks 4043D)	Under oxygen limited conditions	ISO 15985	62.6 ± 6.8% of weight loss after 75 days	7,14–7,73	52 ± 2	–	[152]
PLA films (MTEC)	Under thermophilic oxygen limited conditions	–	90% of weight loss after 90 days	5–7,3	60	–	[153]
PLLA films (NatureWorks 4042D)	Under controlled composting conditions	ASTM D 5988–03	87,5% of biodegradation after 90 days	7,6	27	50	[154]
PLA films (Natureworks, 2003D)	Under simulated aerobic composting conditions	ASTM D5338-15	90% of mineralization and 69,2% of number average molecular weight loss after 140 days	7,78	58 ± 5	45	[155]
PDLA (Natureplast France)	In the solid medium and under aerobic conditions	ASTM G21-90 and ASTM G22-76	7,09% weight loss after 28 days	6–6,5	37 ± 2	–	[156]
PLA films (Natureworks, 2003D)	Aerobic biodegradation by CO_2 analysis in simulated composting	–	100% of mineralization after 90 days	7,9	58	50	[157]
PLA films (Natureworks, 2003D)	Under simulated aerobic composting conditions	ASTM D5338-15	55% number average molecular weight loss after 80 days	7,74	60/58 (±5)	50,15	[47]
PLLA films (Natureworks, 4032D)	Under controlled composting conditions, method by analysis of evolved CO_2	–	90% of mineralization after 100 days	–	58	–	[158]
PBAT							
PBAT films (Bio360)	Under simulated aerobic composting conditions	ASTM D5338	45% of mineralization after 90 days	–	58 ± 1	55	[159]
PBAT films (Ecoflex®)	Under simulated aerobic composting conditions	EN ISO 14855–2:2018	8 ± 1,6% of weight loss after 60 days	7,5	35–60	50–55	[160]
PBAT films (Ecoflex®)	Under mesophilic anaerobic condition by biogas production	–	2,8 ± 0,9% of weight loss after 126 days	7,35	37 ± 2	–	[56]
PBAT films (Ecoflex®)	Under thermophilic anaerobic condition by biogas production	–	8,5 ± 1,9% of weight loss after 126 days	7,65	55 ± 2	–	[56]
PBAT films (Ecoflex®)	Under thermophilic anaerobic conditions	ISO 15985	9.3 ± 2.6% of weight loss after 75 days	7,14–7,73	52 ± 2	–	[152]

Table 2 (continued)

Type of polymer	Biodegradation conditions	Test method	Biodegradation time	pH conditions[a]	Temperature conditions[b] (°C)	Moisture conditions[c] (%)	Reference
PBAT films (Ecoflex®)	Under oxygen limited conditions	ISO 15985	15.6 ± 2.3% of weight loss after 75 days	7,14–7,73	52 ± 2	–	[152]
PBAT films (Organix)	Under simulated aerobic composting conditions	ASTM D5338	60% of mineralization after 90 days	–	58 ± 1	55	[159]
PBAT films (BioAgri®)	Under simulated aerobic composting conditions	–	97% of surface area loss after 126 days	–	20–80	55–65	[161]
PBAT films (Naturecycle)	Under simulated aerobic composting conditions	ASTM D5338	40% of mineralization after 90 days	–	58 ± 1	55	[159]

a), b), c) The conditions inside the biodegradation system; "- " Unknown

because the stereochemical positions of the chiral carbons of the L-lactic acid unit of PLA and the L-alanine unit in the silk fibroin are similar. Thus, microorganisms that can degrade PLA likely identify the L-alanine unit in silk fibroin as an analog of the L-lactate unit in PLA [51].

There are two categories of enzymes involved in the biodegradation process, external and intracellular depolymerases. The degradation process of PLA takes place by secretion of extracellular depolymerase by microorganisms that are stimulated by inducers, in which most inducers have L-alanine units. Then, the polymerase influences the intracellular ester bonds of PLA, producing oligomers, dimers, and monomers, which are taken up by microorganisms through the activity of intercellular enzymes and converted into carbon dioxide, water and methane [52]. Table 3 shows some microorganisms and their enzymes capable of PLA degradation.

Proteases, esterases, lipases, and cutinases induce the enzymatic degradation of polyesters by hydrolysis. For PLA degradation, protease and esterase participate more frequently on that [52].

In addition, studies of PLA-degrading microorganisms have been mainly conducted in controlled laboratory conditions as shown in Table 3. The biodegradability of PLA in the soil takes a long time compared to other biodegradable polyesters because of the limited distribution of PLA-degrading microorganisms in the soil. Thus, the addition of a microbial consortium in the soil can help to accelerate PLA biodegradation [53].

Poly(butylene adipate-co-terephthalate)—PBAT

Poly(butylene adipate-co-terephthalate) (PBAT) is a 100% biodegradable synthetic polymer, based on fossil resources, with high elongation and flexibility [54]. The PBAT is an aromatic aliphatic copolyester that has a good balance between its biodegradability and its physical properties, such as elongation at break and tensile modulus [55]. The aromatic fraction, butylene terephthalate (BT), has excellent physical properties, while the aliphatic fraction, butylene adipate (BA), promotes its degradation through hydrolysis under the effect of microbial enzymes, in which the BA (non-crystalline) structure degrades faster than BT (crystalline) structure [24]. The chemical structure of PBAT is shown in Fig. 1b.

PBAT is also commercially known as Ecoflex®, produced by the company BASF, and widely used in applications such as agricultural materials (mulch film), compost bags, food packaging, laminating materials, organic waste bags, and shopping bags [56].

Table 3 Some microorganisms and enzymes for PLA and PBAT degradation

Strains	Polymer	Sample Source	Degradation conditions	Type of enzyme	pH[a]	T (°C)[a]	Reference
Actinomycete							
A. keratinilytica strain T16-1	PLA	Not specified	Stirred tank bioreactor	-	8.0	60	[162]
Amycolatopsis sp. SO1.1	PLA	Soil	Inoculum with isolated strain	Protease	7	30	[163]
Amycolatopsis sp. SO1.2	PLA	Soil	Inoculum with isolated strain	Protease	7	30	[163]
Actinomadura sp. TF1	PLA	Soil	Liquid culture	Lipase/Esterase	6–8	40–60	[164]
Amycolatopsis sp. SST	PLA	Soil	Inoculum with isolated strain	Protease	7	30	[163]
Amycolatopsis sp. SNC	PLA	Soil	Inoculum with isolated strain	Protease	7	30	[163]
Rhodococcus fascians NKCM2511	PBAT	Soil	Incubation in mineral medium	Esterase lipase	-	25	[55]
Saccharomonospora viridis	PBAT	BAO42836 [e]	Enzyme solution	Cutinase	7.5	30	[165]
Streptomyces sp. APL3	PLA	Soil	Liquid culture	Lipase/Esterase	6–8	40–60	[164]
Thermobifida cellulosilytica	PBAT	ADV92526 [e]	Enzyme solution	Cutinase	7.5	30	[165]
Bacteria							
Bacillus licheniformis	PLA	P4860 [b]	Enzyme solution	Protease	8.2	22	[166]
Bacillus pumilus NKCM3101	PBAT	Soil	Liquid basal medium	Lipase	7	30	[167]
B.pumilus NKCM3201	PBAT	Soil	Liquid basal medium	Lipase	7	30	[167]
B.pumilus NKCM3202	PBAT	Soil	Liquid basal medium	Lipase	7	30	[167]
Chryseobacterium sp. NUl3D48h-1	PLA	Not specified	Inoculum with isolated strain	-	7	30	[168]
Clostridium botulinum	PBAT	AKZ20828 [e]	Enzyme solution	Esterase	7.5	30	[165]
Clostridium hathewayi	PBAT	ALS54749 [e]	Enzyme solution	Esterase	7.5	30	[165]
S. pavanii CH1	PLA	Soil	Submerged culture	Protease	7.0–7.5	30	[169]
Sphingobacterium thalpophilum Y19	PLA	Not specified	Inoculum with isolated strain	-	7	30	[168]
Pelosinus fermentans	PBAT	AIX10936 [e]	Enzyme solution	Lipase	7.5	30	[165]
Pseudomonas aeruginosa BUP2	PLA	Not specified	Inoculum with isolated strain	-	7	30	[168]
Pseudomonas aeruginosa BAC113	PLA	Not specified	Inoculum with isolated strain	-	7	30	[168]
Pseudomonas pseudoalcaligenes	PBAT	DSM 50,188 [f]	Incubated in buffer	Esterase	7–8	50–80	[170]
P. geniculate WS3	PLA	FERS [c]	Soil mixture	Protease	7.38	58 ± 2	[53]
Stenotrophomonas sp.	PBAT	Soil	Inoculum with isolated strain	Lipase	6.3–7.8	27–47	[63]
Fungus							
Aspergillus flavus	PLA	CCUG 2829 [d]	Solid medium and aqueous media	Cellulase	4.2 ± 0.2	30	[171]
Candida rugosa	PLA	Sigma Aldrich	Enzyme solution	Lipase	4.3–8.6	-	[172]
Candida antarctica	PLA	62,288 [b]	Enzyme solution	Lipase	8.2	22	[166]
Cryptococcus sp.	PBAT	MTCC 5455 g	Inoculum with isolated strain	Lipase	-	25	[173]
Knufa petricola	PBAT	MA5789 [h]	Culture in suspension	Lipase/Cutinase	5.5	21	[174]
Sarcynomyces petricola	PBAT	MA5790 [h]	Culture in suspension	Cutinase	5.5	21	[174]
Tritirachium album	PLA	19,133 [b]	Enzyme solution	Proteiase K	8.2	22	[166]

[a]pH and temperature conditions in PLA degrading enzymes;

[b]Purchased from Sigma-Aldrich (St. Louis, MO, USA);

[c]Faculty of Environment and Resource Studies, Mahidol University (Nakhon Pathom, Thailand);

[d]Culture Collection of the University of Gothenburg Research Laboratory;

[e]Extracted from the moss *Sphagnum magellanicum*;

[f]obtained from Leibniz-Institute DSMZ-German Collection of Microorganisms and Cell Cultures in freeze-dried form;

[g]maintained on potato dextrose agar (PDA);

[h]obtained from the ACBR fungal culture collection of the University of Natural resources and Life Sciences, Vienna, Austria; "- " Unknown

PBAT Mechanical Properties

Ecoflex® is a hydrophobic biodegradable polyester with excellent film forming ability, but its low strength and low heat resistance do not recommend it for many applications [57].

Typical values for the mechanical properties of PBAT are listed in Table 1. Compared to PLA, the mechanical properties of PBAT are shown to be more flexible, with the elongation at break over 600%.

The mechanical properties of PBAT are affected by its composition, as the content of terephthalate units increases, the Young's modulus increases, while the elongation at break decreases. Molar mass also affects the mechanical properties of PBAT, because with increasing molar mass, tensile strength increases, and elongation at break also decreases [58].

PBAT Biodegradation Properties

Biodegradation of PBAT also occurs through hydrolysis under the effect of microbial enzymes, in which the amorphous BA structure degrades faster than the crystalline BT structure. PBAT undergoes hydrolytic degradation due to the cleavage of ester bonds and the reaction between water and carbonyl groups located in the vicinity of the benzene rings [24]. Some biodegradation results of PBAT are summarized in Table 2.

Through the data summarized in Table 2, it is possible to notice that PBAT takes longer to degrade than PLA, despite PBAT being known for its wide use in agriculture due to its short degradation rate, which is 6 weeks in the soil [59]. The degradation rate of PLA being higher than that of PBAT was also observed in the study of Ren et al. [60].

The depolymerization of PBAT by soil and compost microorganisms has been studied in recent years. Enzymes with PBAT hydrolytic activity are mostly originating from terrestrial *Actinomycetes* and *fungi* [61]. Some enzymes that can degrade PBAT have been identified among the extracellular carboxylic ester hydrolases, such as esterases, lipases, and cutinases [62]. Table 3 is also summarized some microorganisms and their enzymes capable of degrading PBAT.

There are a few types of PBAT degrading microorganisms, including mainly *Sphingopyxis ginsengisoli, Bacillus pumilus, Pseudomonas pseudoalcaligenes, Cryptococcus,* and *Trichoderma asperellum*, which these bacteria have some disadvantages, such as low degradation rate, and there are few studies that assess whether they can degrade or metabolize the degradation products of PBAT. These products, for example, terephthalic acid and adipic acid, can change the pH of the environment and the community structure of environmental microorganisms, as well as cause physiological toxicity in microorganisms and plants [63].

PLA/PBAT Blend

Some biodegradable polymers are used to modify the limitations of PLA, such as PBAT. PBAT is one of the most attractive polymers for hardening PLA, as PBAT/PLA blends reveal a significant improvement in flexibility and processability [64]. PLA/PBAT blends demonstrate excellent physical–chemical and mechanical properties and can be used in various applications in the medical, industrial, and packaging sectors [65].

In terms of transparency, neat PLA films are more transparent than neat PBAT films, as exposed in the study by [66]. Due to the poor light transmission of PBAT, the clarity of the PLA/PBAT composite films was decreased when adding PBAT to PLA. The color of PLA/PBAT composite films became more off-white with the increase of PBAT contents.

PLA and PBAT produce immiscible blends and depending on composition and processing methods can exhibit matrix-droplet or co-continuous morphology. Immiscible blends with a morphology of smaller droplets and well dispersed in the matrix phase show significantly improved properties. Therefore, coalescence of PBAT droplets after further processing needs to be controlled [30].

Compatibilization of PLA/PBAT Blend

PLA/PBAT blends are highly promising materials due to the considerable mechanical strength of PLA and the extreme rigidity of PBAT (when well compatibilized), because although PBAT has carbonyl groups similar to PLA, the low interfacial adhesion and macro-phase separation between these two polyesters make them immiscible [18]. The physical properties and dispersibility behavior of the immiscible heterogeneous blend can be improved by compatibilization through physical or chemical interaction between the components [67]. Also, irradiation can be used to improve the compatibility between immiscible polymers in a blend [68].

Table 4 summarizes the effects of various types of compatibilizers in PLA/PBAT blends showing the ratios of the tensile strength (σ), of the elongation at break (ε), and of the impact strength (a) for both compatibilized (comp) and non-compatibilized (neat) blends, $\sigma_{comp}/\sigma_{neat}$, $\varepsilon_{comp}/\varepsilon_{neat}$, and a_{comp}/a_{neat}, respectively.

As reported in Table 4, several compatibilizing agents are shown to be efficient in the interfacial adhesion of the blend, which leads to an increase in tensile strength, elongation at break, and impact strength of the PLA/PBAT blend.

Wang et al. [67] studied ADR, a compatibilizer with several epoxy groups and high reactivity, used as a

Table 4 Ratios of tensile strength ($\sigma_{comp}/\sigma_{neat}$), elongation at break ($\varepsilon_{comp}/\varepsilon_{neat}$), and impact strength ($a_{comp}/a_{neat}$) of compatibilized and neat PLA/PBAT blends for various compatibilizers

Blend Composition (PLA/PBAT)	Compatibilizer	$\sigma_{comp}/\sigma_{neat}$	$\varepsilon_{comp}/\varepsilon_{neat}$	a_{comp}/a_{neat}	Reference
90/10 wt/wt	0.75 wt% of Joncryl ADR-4370S (ADR)	107	116	113	[67]
80/20 wt/wt	0.75 wt% of Joncryl ADR-4370S (ADR)	113	118	107	[67]
70/30 wt/wt	0.75 wt% of Joncryl ADR-4370S (ADR)	120	103	142	[67]
60/40 wt/wt	0.75 wt% of Joncryl ADR-4370S (ADR)	128	120	580	[67]
70/30 wt/wt	0.5 phr of epoxidized soybean oil (ESO)	122	115	111	[69]
70/30 wt/wt	1 phr of epoxidized soybean oil (ESO)	116	161	161	[69]
70/30 wt/wt	3 phr of epoxidized soybean oil (ESO)	117	230	340	[69]
70/30 wt/wt	5 phr of epoxidized soybean oil (ESO)	125	628	417	[69]
80/20 wt/wt	3 wt% of epoxy-cardanol prepolymer (ECP)	107	365	-	[175]
80/20 wt/wt	3 wt% of Joncryl ADR-4300 (ADR)	127	246	-	[175]
90/10 wt/wt	3 wt% of PLA-grafted-MA	201	233	113	[84]
90/10 wt/wt	5 wt% of PLA-grafted-MA	158	246	191	[84]
50/50 wt/wt	10 phr of $CaCO_3$ and 5 phr of PLA 150 kGy gamma-irradiated	133	097	-	[68]
35/65 wt/wt	10 phr of $CaCO_3$ and 5 phr of PLA 150 kGy gamma-irradiated	117	098	-	[68]
18/82 wt/wt	10 phr of $CaCO_3$ and 5 phr of PLA 150 kGy gamma-irradiated	160	094	-	[68]
90/10 wt/wt	3 wt% of toluenediphenyl diisocyanate (TDI) based on PBAT	104	122	116	[176]
40/60 wt/wt	0.3 phr of Joncryl ADR-4368 (ADR)	108	077	110	[70]
40/60 wt/wt	0.5 phr of Joncryl ADR-4368 (ADR)	105	081	113	[70]

"- " Unknown

compatibilizer in PLA/PBAT blends. Different ratios of PLA and PBAT with ADR were evaluated in terms of surface morphologies. The non-compatibilized PLA/PBAT blends presented an island-like structure, and the particle size of the dispersed phase increased with the increase of the PBAT content due to the low compatibility and interfacial adhesion between PLA and PBAT. With the addition of the ADR compatibilizer, the particle size of the PBAT dispersed phase significantly decreased and these particles were better mixed in the PLA matrix due to the improvement of the interfacial interaction.

In Han et al. [69], epoxidized soybean oil (ESO) used as a compatibilizer for the PLA/PBAT blend using the reaction between an epoxy group and a hydroxyl group, forming a chemical bond between the PLA and PBAT phases and the microstructure of the quenched fracture surface of the PLA/PBAT was obtained by scanning electron microscopy. Tiny round particles were observed that correspond to the dispersed PBAT phase, while the matrix is the continuous PLA phase. The high definition of the boundary with the surrounding continuous phase indicates poor compatibility of PLA and PBAT in the absence of the compatibilizing agent. Further, the PBAT particles gradually become smaller as the amount of ESO compatibilizer increases, and the boundary between the particles and the matrix gradually becomes blurred. Specifically, 5, 7 and 9 phr of ESO already show an emulsification behavior of the two-phase interface, in which they appear to be completely fused. Therefore, through microscopy, the excellent compatibilization effect of ESO in PLA/PBAT blends is observed.

And there are some studies that report the increase of compatibility of polymers with PLA using Joncryl as a compatibilizing agent, which exhibits results in improvement of rheological, thermal, and mechanical properties, for example, increased melt storage modulus and viscosity [70], higher improvements in impact strength and ductility [71], and an increased shear viscosity, a higher melt strength and an induction of strain hardening due to the formation of branched chains and/or even crosslinking [72].

The most common approach to compatibilizing multiphase polymers is through the addition of compatibilizing agents. However, high-energy radiation, such as gamma rays and electron beams (e-beam), has been gaining much interest as it has potential use in increasing interfacial compatibility via interaction and recombination of macromolecular radicals generated during radiation exposure. These highly energetic irradiations produce bond cleavages and free radicals that promote molecular reactions and close interactions between the polymer chains at the blend interfaces [73, 74].

Cardoso et al. [68] studied PBAT/PLA blends reinforced with bio-calcium carbonate from avian eggshells and compatibilized with PLA gamma-radiated to 150 kGy, and further assessed for SEM essays, as shown in Fig. 2. Neat PLA has an irregular dispersion in its morphology (island-phase

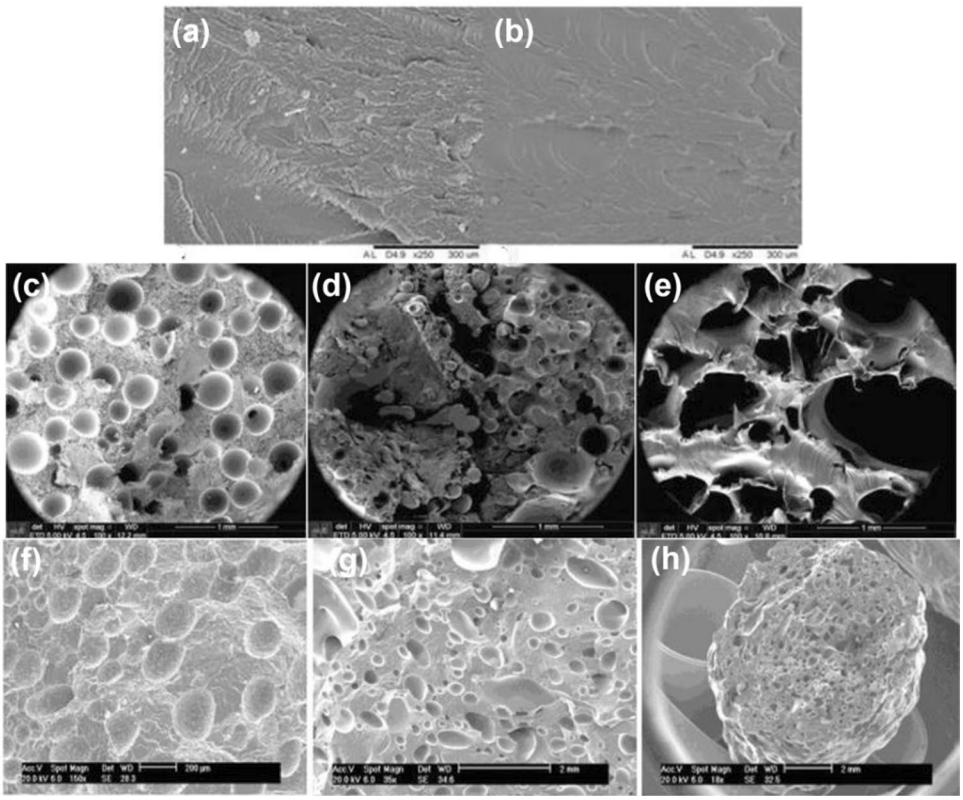

Fig. 2 SEM micrographs: **a** 500 X magnification for neat PLA; **b** 500 X magnification for neat PBAT; **c** 100 X magnification for PBAT/PLA, 82/18; **d** 100 X magnification for PBAT/PLA, 65/35; **e** 100 X magnification for PBAT/PLA, 50/50; **f** 150 X magnification for PBAT/PLA/CaCO3/PLA 150 kGy gamma-irradiated; **g** 35 X magnification for PBAT/PLA/CaCO3/PLA 150 kGy gamma-irradiated; **h** 18 X magnification for PBAT/PLA/CaCO3/PLA 150 kGy gamma-irradiated (Reprinted (adapted) with permission from IntechOpen) [68]

type), while neat PBAT has a continuous phase (sea-phase type), as can be seen in Figs. 2a, b. When mixed, the higher the concentration of PBAT in the blend, the easier the miscibility between PBAT and PLA, as shown in Figs. 2c, d, e. And finally, the addition of 150 kGy gamma-irradiated PLA contributed to an effective reinforcement distribution of 125 µm of bio-calcium carbonate in the blend compositions and build-up of structural foams, as seen in Figs. 2f, g, h.

However, few studies in the literature evaluate the compatibilization of the PBAT/PLA blend by gamma rays or electron beam radiation. Other works were carried out using irradiation to increase the compatibility of polymeric blends. Table 5 summarizes some formulations of polymeric blends irradiated as a physical compatibilizing agent.

These polymers irradiated with gamma rays, shown in Table 5, showed improvement in the interfacial adhesion of the blend, proving the efficiency of this method in the compatibilization of immiscible blends. In which, the dose rate and the presence of coupling agents can influence the compatibilization of the blend.

Aldas et al. [75] evaluated the compatibilization of PLA/PBAT blends with gum rosin (GR), a natural additive that can act as a plasticizer, providing solubilization and compatibilization effects in biodegradable blends. The visual aspect of the films obtained for PLA/PBAT blends (80/20 wt/wt) with 0 to 20 phr of GR, neat PLA, neat PBAT, and PBAT with 10 phr of GR were evaluated. It is possible to observe the high transparency of the neat PLA film. The addition of 20% by weight of PBAT showed some loss of transparency, as neat PBAT has more opacity. The higher incorporation of GR also led to a partial decrease in the high transparency of the PLA, which was more pronounced with increasing the amount of GR. The incorporation of GR in the PBAT was practically imperceptible in the transparency of the sample. That is, although GR can be used to improve the toughness of PLA/PBAT formulations, this adhesion does not increase the transparency of the blend.

Biodegradation of PLA/PBAT Blend

In recent years, PLA/PBAT blend has gained importance among biodegradable materials in the fields of food and agriculture due to its excellent mechanical properties and biodegradability, which researchers usually analyze by landfilling and composting [76]. PLA/PBAT can be biodegraded by certain microorganisms and their enzymes secreted into the environment. Protease and lipase have significant degrading effects on PLA and PBAT, respectively as also reported by [77].

In the study of Inga-Lafebre et al. [78], the biodegradation of neat PLA, neat PBAT, and PLA/PBAT (80/20 w/w) blend with different compatibilizing agents (3 wt% of Amberyl M-15A (A15) and 3 wt% of Amberyl MP-30 (A30)) were analyzed in composting in a convection oven for 90 days.

Table 5 Formulations of blends and composites irradiated by electron beam and gamma rays

Polymer Blends	Proportions	Irradiation	Coupling agent	Characterizations	References
PLA/Lignin	95/5; 80/20	Electron beam at 30, 60, and 90 kGy	Triallyl isocyanurate (TAIC) at 0 and 3 phr	Mechanical properties, FTIR, DSC, SEM, XRD, and hydrolytic degradation	[177]
EVA/tPA/SP[a]	70/30/3(5)	Electron beam 50 to 250 kGy with 10 kGy/pass	–	Tensile properties, FTIR, DSC, SEM, DMA, and oil swelling test	[178]
PLA/Bamboo	95/5; 90/10	Electron beam at 30 kGy	Epoxide silane (ES) at 0, 5, and 10 phr	Mechanical properties, FTIR, DSC, SEM, XRD, and hydrolytic degradation	[179]
LDPE/EVA	90/10; 75/25; 50/50; 25/75; 10/90	Electron beam at 78, 130, and 200 kGy with 10 kGy/pass	–	Mechanical properties, SEM, and gel content	[180]
PLA/Flax	95/5	Gamma irradiation at 5, 10, 15, and 20 kGy	Triallyl isocyanurate (TAIC) at 3 wt%	Mechanical properties, TGA, Water absorption, Swelling morphology, and fraction of gel	[181]
PLA/PBAT	80/20; 20/80	Electron beam at 10, 40, and 90 kGy	Triallyl isocyanurate (TAIC) at 3 wt%	Determination of uncrosslinked fraction, FTIR, DSC, and molecular weight	[182]
PBS/TPS	50/50	Electron beam at 5, 13, and 26 kGy	–	Mechanical properties, FTIR, DSC, TGA, SEM, Gas chromatography, microbiological analysis, and degradation	[183]
PLA/PCL	90/10; 70/30	Electron beam at 5, 10, 20, 50, 100, and 200 kGy	Glycidyl methacrylate (GMA) at 3 phr	Mechanical properties, FTIR, SEM, Rheological properties, thermal stability, and biodegradability	[184]
PLA/PEGM	80/20	Electron beam at 20, 60, and 100 kGy	–	Mechanical properties, HDT, DSC, SEM, and hydrolytic degradation	[185]
PLA/PHBV	50/50	Gamma irradiation at 25, 50, and 100 kGy	Maleic anhydride (MA) at 0,29 wt%	FTIR, Molecular weight, DSC, TGA, Nanoindentation test, SEM, and PCFC	[186]
PBAT/Starch	65/35	Gamma irradiation at 25 kGy	–	TGA, DSC, XRD, and SEM	[187]

[a]tPAC = Ternary polyamide copolymer of polyamide 6, 66 and 1010 (30/30/40 wt%) and SP = Sepiolite filler.; "- "Unknown

The weight loss results after 90 days reached the highest degradation rate for neat PLA (0% of residual weight) and the lowest for neat PBAT (79,3% of residual weight), while reasonable biodegradation values were obtained for the blends (16,6% for the blend with no compatibilizing agent, 26,4% with A15 and 23,7% with A30) which indicates that the compatibilizing agent in addition to helping to improve mechanical performance, does not affect its biodegradation capability.

Harada et al. [79] analyzed the biodegradation of the PBAT/PLA (46/54 wt/wt) blend (A0) and composites with 2% of carbon black (A1), 2% carbon black, and 4% of organic fertilizer (A2), 2% of carbon black and 2% of silica from rice husk ash (A3), and all together (A4), in simulated soil at room temperature (25 ± 3 °C), in 10 to 40% C:N ratios and pH = 7.0 ± 0.5 for 12 months. It was possible to identify that PBAT/PLA blend after 12 months reached about 35% of weight loss. The incorporation of carbon black (A1) in this mixture showed an influence to accelerate soil degradation. But the addition of most influential fillers to accelerate the mass loss was organic fertilizer (A2), about 85% of weight loss, and rice husk silica (A3), about 80% of weight loss. However, together (A4), this effect was less significant.

And in the study of Osman et al. [28], the biodegradation of PLA/PBAT (85/15 wt/wt) blend with 1.0 wt% of Sodium Montmorillonite (Na-MMT), octadecylammmonium and Sodium Montmorillonite (ODA-MMT), dimethyl dioctadecyl ammonium and Sodium Montmorillonite (DDOA-MMT) and commercial clay Closite 20A (C20A) were analyzed in simulated soil for 12 weeks. The PLA/PBAT blend showed 8,76% of weight loss at 12 weeks. The addition of Na-MMT showed the highest weight loss after 12 weeks (9.02%). On the other hand, the addition of ODA-MMT, DDOA-MMT, and C20A tends to reduce the

biodegradation rate in the samples, 7.96%, 7,62%, and 7,41% after 12 weeks, respectively.

Studies show that the biodegradation rate of the PLA/PBAT blend is lower than that of the neat PLA and PBAT [24, 80]. The inclusion of PBAT affects the molecular weight retention rate of PLA, which demonstrates that the PBAT content is an important factor in the PLA/PBAT composite degradation rate. Elevating the PLA content in the composite leads to a higher increase in the O/C content ratio after degradation [24]. And the higher content of PBAT is in the blend, the higher is the degradation of the PLA/PBAT blend [81].

Manufacturing

Manufacturability development for batch and mass production is one of the key aspects of product development due to application capability and commercial advantages. Manufacturing methods such as films, foams, and fused deposition modeling (FDM) are well-studied for the PLA/PBAT blends [68, 82–86].

Films of PLA/PBAT blends have application in the areas of medicine, industry, and packaging (such as food packaging and agricultural commodities), they have low density, high toughness, and high-performance biodegradable plastic packaging films. However, PLA has limitations for use as a packaging film owing to its poor performance of mechanical and physical properties such as being brittle. It has been blended with other polymers of high elasticity such as PBAT to improve these properties [29, 65, 87, 88].

Foams of PLA/PBAT blends have applications in packaging, floating materials, paddings, shields for reducing noise, shoes, and others. They have low density, insulating capability, and energy absorption. Foaming PLA is a challenging due to its low melt strength, melt viscosity and elasticity, and poor crystallization. The collapse and merging of cells often occur during the foaming process, particularly in extrusion foaming. The use of PBAT improves the foaming process and cell morphology [68, 86].

In addition, fused deposition modeling of PLA/PBAT blends is mostly used for 3D printing technology, like large-scale wastewater treatment. Have a simple operation, high performance of printing products and is convenient to adjust and control the structure. Due to the layering caused by the printing method, the mechanical properties of the printed products largely depend on the printing direction of the blend [82, 85].

As previously discussed, PLA /PBAT blends are immiscible [18]. But, there is very little information on the blown film processing of PLA compounded with PBAT. Hougdilokkul et al. (2015) evaluated the properties of PLA/PBAT from a blown film process, from a PLA/PBAT blend, with a weight ratio of 80:20, together with peroxide as a reactive agent. Figure 3 shows the blown film processing of neat PLA, PBAT, and the reactive blend of PLA/PBAT (P0.02). Blowing neat PLA was difficult, and the bubble shape was unstable due to the low melt strength of PLA. The resulting film had a large variety of dimensions and thicknesses. The film was transparent as PLA was amorphous and had a low crystallization rate. In the case of neat PBAT film processing, it was easier to blow. On the other hand, the PBAT film was stuck together after conveying into the nip roll. In the case of PLA/PBAT blends with and without peroxide, the films could be processed more easily when compared to neat PLA.

Pang et al. [90] reported three parameters that characterize the cell structure: cell size, cell density, and expansion ratio. Foamed plastics, also called cellular polymers or expanded plastics, can be made from almost any type of polymer: the type of polymer determines whether the resulting foam will be hard and rigid or soft and flexible. Cardoso et al. [68] studied PBAT/PLA foams reinforced with bio-calcium carbonate from avian eggshells (125 µm particle size) and compatibilized with gamma radiation at

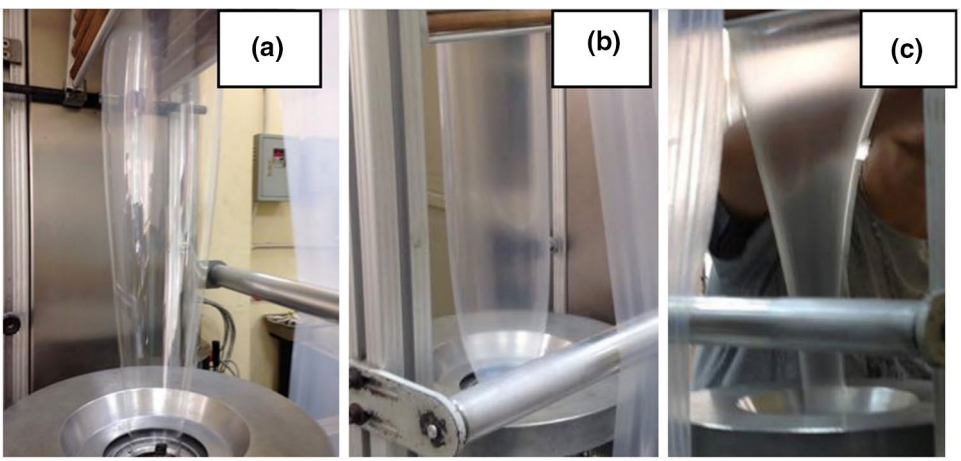

Fig. 3 Comparison of the illustration between **a** Neat PLA, **b** P0.02 and **c** Neat PBAT (Reprinted with the permission of IOP) [89]

150 kGy. Figure 4 foamed samples obtained from a 4 mm die extruder and final specimens are shown. The higher the PBAT concentration in PLA/PBAT blends, the easier the miscibility between both PBAT and PLA. And the addition of PLA gamma-irradiated at 150 kGy contributed to an effective distribution of bio-calcium carbonate (125 µm) reinforcement in PBAT/PLA compositions and the buildup of structural foams.

Prasong [91] prepared superior toughened biodegradable polymer blend nanocomposites from PLA, PBAT, and nano talc for alternative materials in 3D printing by FDM. The printability and the dimension stability of the 3D printing products were evaluated from the vertical dumbbell and the overhang test specimens with PLA/PBAT blend samples in different proportions (100/0, 90/10, 80/20, 70/30, and 60/40 wt%) and with the addition of nano talc at 0–40% by weight. PLA/PBAT blends up to 20% by weight PBAT show good formation, in the 70/30 blend a rough surface appeared, and in the 60/40 blend, the printing was not completed. This was attributed to the flexibility of the PBAT and the high value of the volume expansion coefficient at the printing temperature. In despite of that, when added nano talc significantly the printability of the PLA/PBAT blend improved in all formulations, especially in the 60/40 blend. And the addition of the nano talc ratio on the overhang test products for the 70/30 blend revealed that dimensional stability was improved by increasing the content of nano talc.

Nanocellulose

Cellulose nanoparticles are derived from various natural cellulosic sources and have great potential as alternatives to synthetic nanoparticles and unique properties resulting from their structural and chemical surface [92]. Cellulose is the most abundant biodegradable polymer available and is mainly extracted from plants such as wood, hemp, cotton, and linen, but it can also be produced by microorganisms such as fungi and bacteria with the same chemical composition, differing only in the degree of polymerization, purity and other characteristics [39]. Cellulose has excellent mechanical properties, such as tensile and flexural strength, tensile and flexural modulus, in addition to being low cost, as it is available in different resources and from abundance in nature [93, 94].

Cellulose is a long-chair linear polysaccharide composed of β-D-glucopyranose ($C_6H_{12}O_6$) units formed by β-1,4-glycosidic bonds, in which the basic unit, called cellobiose ($C_{12}H_{22}O_{11}$), which is nothing more than that two β-D-glucopyranose units, is rich in -OH groups, providing a medium for intermolecular and intramolecular hydrogen bonds, forming the elementary fibrils [95, 96],as shown in Fig. 1c. Materials based on this biopolymer have been widely used in various applications, such as textiles, food, medicine, paper, engineering materials, biofuels, and composites [97].

In addition to the possibility of being obtained from various sources, such as wood and plants, bacteria, algae, and even marine animals, such as tunicates, cellulose has several morphological forms in different dimensions, shapes, crystallinity, and physicochemical properties, among them, are cellulose fibers, cellulose filaments, cellulose crystals, and cellulose micro/nanofibrils [98].

Fibers extracted from wood and plants, although they have the same chemical structure, have a different structural organization, also varying in the proportion of cellulose, hemicellulose, and lignin [98]. The cellulose content in plants is generally 30–75% and in wood is 40–50% [98].

Nanocellulose can be characterized into two main groups: nanocrystalline cellulose (CNC) and nanofibrillated cellulose (CNF). Nanocrystalline cellulose is extracted from cellulose through acid hydrolysis and it is less flexible compared to CNF due to its greater crystallinity. Nanofibrillated cellulose, on the other hand, is commonly obtained by mechanical treatment, presenting an entangled network structure with flexible nanofibers and lower crystallinity [99, 100].

For CNCs extraction, concentrated mineral acid, such as sulfuric acid, is wildly used for hydrolysis to remove the amorphous region containing lignin and non-cellulosic

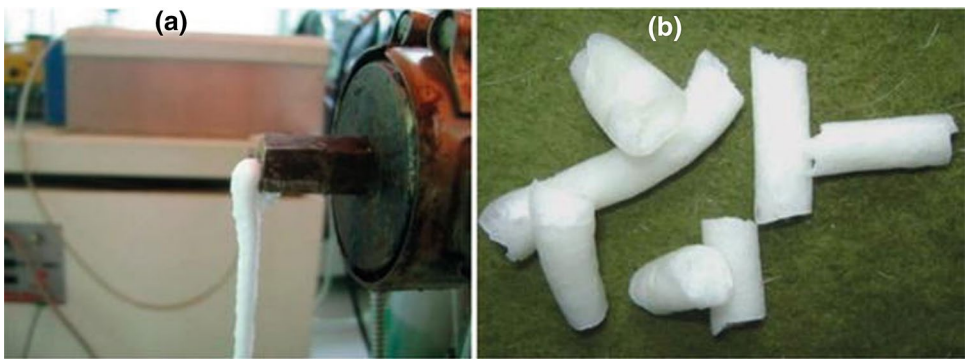

Fig. 4 Structural foams: **a** extruded foams from a 4 mm die extruder; **b** cylinder structural foams, of approximately 400 kg.m^{-3} density (Reprinted with permission from IntechOpen) [68]

components [101–103]. The hydronium ions produced during the acid treatment can penetrate the amorphous region, allowing the cleavage of 1,4–glycosidic linkages within the cellulose chain and breaking the strong network of hydrogen bonds between the cellulose chains [103]. And for CNFs extraction, there are mainly two mechanical methods, namely conventional and non-conventional methods. Conventional methods include homogenization, milling, etc., while non-conventional ones include mixing, cryo-crushing, ultrasonication, and others [104]. Figure 5 represents a schematic isolation of CNC and CNF showing their structural differences by TEM images.

CNCs have a length of 100 to 600 nm and a diameter of 2 to 20 nm, whereas the CNFs are longer than 1000 nm and 5 to 30 nm in diameter [105]. CNCs and CNFs have different costs, morphologies, lengths, crystallinities, and surface charges. CNC films have better optical transparency than CNF films due to the smaller size of CNCs. On the other, the amorphous regions of CNFs can help to absorb more deformation, allowing CNF nanocomposites to have a higher tensile strain to failure compared to the CNC nanocomposite [106].

Natural fibers are considered potential material to be used as reinforcement materials in composite products, and the mechanical properties of plant fibers depend on factors such as physical, chemical, morphological, and geometric characteristics [107].

Some fiber characteristics can change the mechanical properties observed in the final composite as for: fiber length, fiber weight ratio, fiber orientation, fiber and matrix selection, manufacturing process, and interfacial interaction between fiber and matrix [108].

Many studies assess the increase in mechanical properties with the addition of natural fibers in PLA, PBAT, and their blends. Table 6 summarizes some results of mechanical properties reported in the literature for PLA, PBAT, and PLA/PBAT blend reinforced with natural fibers.

It is possible to notice in Table 6 that PLA/fiber composites have greater mechanical properties compared to PBAT/fiber composites. Graupner et al. [109] report that this phenomenon could be based on a combination of poor fiber/matrix adhesion and very high elongation of the PBAT. PLA composites, on the other hand, show the opposite trend. It is assumed that the average fiber elongation is greater than that of PLA, leading to improved tenacity of the composite.

During the last few years, cellulose fiber reinforced polymers have gained great importance among advanced engineering materials and these composites have a wide range of applications [110]. The addition of natural fibers and cellulose derivatives as reinforcing agents is an effective way to improve the polymer properties and lower its final price, maintaining the biodegradability of the matrix [54].

The effect of adding cellulose fibers on the biodegradation of composites with PLA, PBAT and PLA/PBAT blend is studied by some authors. In the work of Xu et al. [111], the percentages of degradation of cellulose, PLA, and Cellulose/PLA films (C/PLA) as a function of burial time in soil were analyzed. C/PLA films were more degradable than neat cellulose and neat PLA films. The C/PLA (1:1) film was completely degraded when buried for up to 45 days, while for neat cellulose and neat PLA the degradation percentage was 81% and 68%, respectively, when buried in the soil for 90 days.

Different stages of surface morphological characteristics of PBAT composites with microcrystalline cellulose subjected to different burial periods were studied in the work of Giri et al. [112]. Compared to the highly ductile nature of PBAT, on composting soil, both PBAT and its composites become quite brittle. After 4 months of composting, the samples became very brittle, and as the amount of

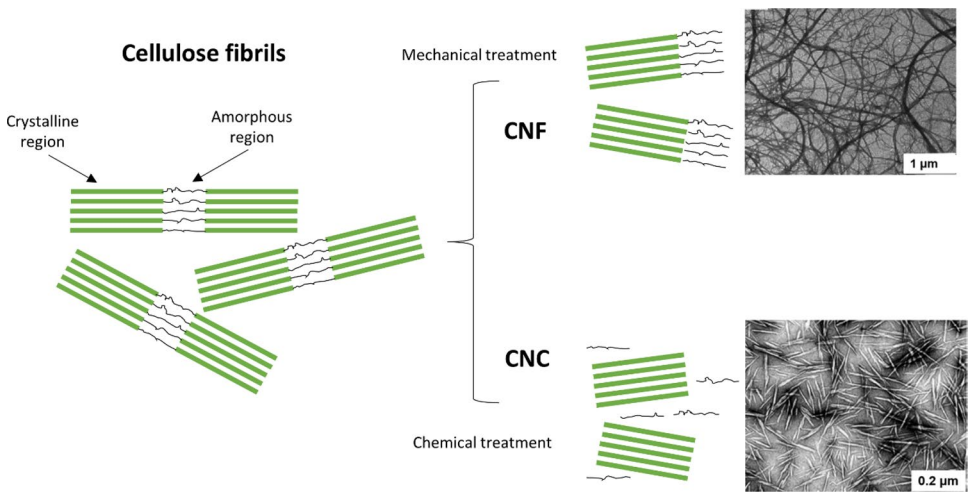

Fig. 5 General scheme of isolating nanocrystalline cellulose (CNC) and nanofibrillated cellulose (CNF). TEM micrographs adapted with permission from [140]. (Reprinted with permission from MDPI)

Table 6 Mechanical properties of PLA, PBAT, and PLA/PBAT composites reinforced with some natural fibers

Components	Fiber (%)	Processing	Tensile strength (MPa)	Tensile modulus (GPa)	Flexural strength (MPa)	Flexural modulus (GPa)	Impact strength (kJ/m^2)	References
PLA								
PLA/Agave (untreated)	40	Extrusion and press molding	49.67 ± 2.46	2.9	96	3.77 ± 0.01	7.88 ± 0.29	[188]
PLA/Agave (NaOH-treated)	40	Extrusion and press molding	53.97 ± 1.07	2.8	98.8	3.81 ± 0.02	6.76 ± 0.32	[188]
PLA/Agave (Enzyme-treated)	40	Extrusion and press molding	57.19 ± 0.90	2.9	98.5	3.82 ± 0.01	6.55 ± 0.27	[188]
PLA/Aloe vera (untreated)	30	Extrusion-Injection molding process	44.7	3.5	74	5.2	40 J/m	[189]
PLA/Aloe vera ($NaHCO_3$-treated)	30	Extrusion-Injection molding process	52.4	7.30	91.2	7.01	33.4 J/m	[189]
PLA/Bagasse (untreated)	30	Extrusion-Injection molding process	60.3 ± 5.8	2.03 ± 0.33	85 ± 16	5.06 ± 0.19	2.86 ± 0.25	[190]
PLA/Bagasse (Silane-treated)	30	Extrusion-Injection molding process	80.2 ± 6.7	2.57 ± 0.25	111 ± 19	5.24 ± 0.13	3.58 ± 0.27	[190]
PLA/Flax	30	Compression molding	52.35	2.25	75.54	2.15	56.64 J/m	[191]
PLA/Hemp	25	Extrusion-injection molding	54.31 ± 7.25	1.14 ± 0.11	99.25 ± 9.42	2.06 ± 0.21	–	[192]
PLA/Hemp	25	Injection molding	47.63 ± 5.62	1.42 ± 0.15	95.46 ± 7.48	2.34 ± 0.15	–	[192]
PLA/Jute	30	Compression molding	45.67	2.01	57	1.76	37.57 J/m	[191]
PLA/Jute/Flax	15/15	Compression molding	49.35	2.80	80.50	2.25	61.46 J/m	[191]
PLA/Kenaf (untreated)	2.5	Fused deposition modeling	40	0.87 MPa	59.30	1.9 MPa	–	[193]
PLA/Kenaf (Silane-treated) [a]	2.5	Fused deposition modeling	57.85	1.2 MPa	84.22	3.17 MPa	–	[193]
PLA/Ramie	30	Compression molding	59.3	–	136.8	–	8.3	[194]
PLA/Sisal (untreated)	20	Hand lay-up technique and static compression	24.71 ± 1.67	1.42 ± 0.08	55.12 ± 3.31	2.24 ± 0.17	20.22 ± 1.47	[195]
PLA/Sisal (NaOH-treated)	20	Hand lay-up technique and static compression	34.57 ± 2.01	2.11 ± 0.07	72.70 ± 4.45	3.52 ± 0.20	23.55 ± 1.98	[195]

Table 6 (continued)

Components	Fiber (%)	Processing	Tensile strength (MPa)	Tensile modulus (GPa)	Flexural strength (MPa)	Flexural modulus (GPa)	Impact strength (kJ/m^2)	References
PLA/Sisal (PLA-coated)	20	Hand lay-up technique and static compression	36.78 ± 2.21	2.32 ± 0.15	81.33 ± 5.45	3.67 ± 0.22	25.75 ± 2.01	[195]
PLA/Wood	40	Fused deposition modeling [b]	35.9	0.81	70.4	2.70	–	[196]
PBAT								
PBAT/Bamboo (untreated)	50	Injection molding	15 ± 1.5	0.69 ± 0.05 MPa	–	–	6.7 ± 0.8	[197]
PBAT/Bamboo (compatibilized) [c]	50	Injection molding	28.6 ± 1.6	1.29 ± 0.08 MPa	–	–	45.6 ± 3.8	[197]
PBAT/Curauá (Hydrolyzed)	5	Mixed and extruded	15.5 ± 3.2	84.0 ± 9.0 MPa	–	–	–	[198]
PBAT/Curauá (Acetylated)	5	Mixed and extruded	19.4 ± 4.0	73.2 ± 12.1 MPa	–	–	–	[198]
PBAT/EFB [d]	20	Compression molding	5.5	0.08	9.7 ± 0.44	0.21	–	[199]
PBAT/EFB [d]	40	Compression molding	7.5	0.21	10.3 ± 0.63	0.46	–	[199]
PBAT/Flax (non-woven)	40 [e]	Compression molding	6.16	0.20	7.1	0.38	9.4	[200]
PBAT/Flax (woven) [f]	40 [e]	Compression molding	28.5	0.36	12.1	1.12	13	[200]
PBAT/Hemp (untreated)	40	Compression molding	111 ± 14	2.43 ± 0.25	–	–	–	[201]
PBAT/Hemp (NaOH-treated)	40	Compression molding	97 ± 12	4.80 ± 0.55	–	–	–	[201]
PBAT/Hemp (NaOH-treated with npMCO) [g]	40	Compression molding	76 ± 14	5.48 ± 0.28	–	–	–	[201]
PBAT/Peach palm	10	Extrusion-injection molding	16.5	0.13	–	–	–	[13]
PBAT/Peach palm	20	Extrusion-injection molding	13.7	0.23	–	–	–	[13]
PBAT/Peach palm	30	Extrusion-injection molding	13.6	0.32	–	–	–	[13]
PLA/PBAT								
(70/30)/Buckwheat	10	Extrusion-injection molding	38.0 ± 0.7	2.39 ± 0.03	65.3 ± 7.5	2.25 ± 0.45	4.2 ± 0.3	[202]
(70/30)/Corn	30	Compression molding	10.7	–	16.5	–	2.33	[203]
(90/10)/Flax	54 h	Compression molding	59.6 ± 5.5	4.46 ± 0.47	89.2 ± 8.3	6.64 ± 0.10	7.9 ± 1.1	[204]
(80/20)/Flax	54 h	Compression molding	52.0 ± 5.2	5.69 ± 0.24	74.7 ± 2.9	6.37 ± 0.15	10.4 ± 1.2	[204]
(70/30)/Flax	54 h	Compression molding	61.0 ± 3.3	4.58 ± 0.04	65.8 ± 4.7	5.57 ± 0.24	9.0 ± 0.4	[204]

Table 6 (continued)

Components	Fiber (%)	Processing	Tensile strength (MPa)	Tensile modulus (GPa)	Flexural strength (MPa)	Flexural modulus (GPa)	Impact strength (kJ/m^2)	References
(87/13)/Hemp	40	Extrusion-injection molding	57.5	–	84	3.9	42.9 J/m	[205]
(90/10)/Kenaf	10	Compression molding	36.69	1.15	37.50	3.84	191.97 J/m	[206]
(90/10)/Kenaf	30	Compression molding	28	0.93	31.5	3.35	116 J/m	[206]
(90/10)/Kenaf	50	Compression molding	17.7	0.42	17.11	3.11	39 J/m	[206]
(95/5)/Ramie	30	Compression molding	52	–	101	–	9.4	[194]
(90/10)/Ramie	30	Compression molding	40	–	99	–	11.8	[194]
(85/15)/Ramie	30	Compression molding	27	–	72	–	10.9	[194]
(70/30)/Rice	30	Compression molding	12.5	–	17.8	–	2.7	[203]
(92/8)/Sisal	20	Compression molding	41	1.63 MPa	76	4.09	–	[207]
(92/8)/Sisal	30	Compression molding	40	1.84 Mpa	77	4.34	–	[207]
(92/8)Sisal	40	Compression molding	34	1.97 MPa	62	3.71	–	[207]
(70/30)/Sorghum	30	Compression molding	12.2	–	18.2	–	3.2	[203]
(70/30)/Soybean	30	Compression molding	14.3	–	19.5	–	3.2	[203]
(70/30)/Wood	30	Extrusion-injection molding	60.6 ± 0.7	3.11 ± 0.02	65.2 ± 1.1	4.26 ± 0.06	3.8 ± 0.1	[208]
(86/14)/Wood (treated) [i]	30	Injection molding	43.4 ± 3.8	4.22 ± 0.03	–	4.09 ± 0.03	3.11 ± 0.24	[209]
(71/29)/Wood (treated) [i]	30	Injection molding	40.2 ± 3.1	4.11 ± 0.04	–	3.99 ± 0.04	3.82 ± 0.33	[209]

[a]1.0 wt % silane concentration + 6% alkali concentration kenaf fibre composites;

[b]on-edge orientation printing and 0°/90° layer deposition;

[c]With 2 phr of 4,40-methylenebis(phenyl isocyanate) (MDI) as a reactive compatibilizer to modify the bamboo-flour surface;

[d]Oil palm empty fruit bunch;

[e]Composites laminates were prepared with two layers of fibers placed alternately between three layers of PBAT films in parallel arrays;

[f]PBAT/4 × 4 plain weave flax composites;

[g]macrocyclic oligomers non-purified (npMCOs) were pre-adsorbed onto hemp fibers NaOH-treated by immersing the fibres in a CHCl3 solution (5% wt./v) of npMCOs;

[h]Composites samples were prepared by stacking 6 layers of flax fabric and 5 films of PLA/PBAT;

[i]treated by a titanate coupling agent; "- " Unknown

microcrystalline cellulose increased in the composts, the fragility of the composite became more pronounced.

Ramle et al. [83] analyzed bamboo cellulose incorporated into PLA and PLA/PBAT, and allowed the films under degradation in soil containing abundant nitrogenous bacteria for 15 days. The samples of PLA and PLA/PBAT with 9 wt% of cellulose showed the highest mass loss rates, 12.39%, and 9.69%, respectively. And the neat samples of PLA and PLA/PBAT were the ones with the lowest mass loss rates, 0.57%, and 0.44%, respectively. Therefore, the increase in cellulose content accelerated the degradation of the films beyond the nominal presence of cellulose.

Nanocellulose have a wide range of applications, for example, in packaging [113, 114], nanocomposites in textiles [115], for wastewater treatment [116], in cementitious materials [117], nanocomposites for energy applications [118], and in biomedical and biosensing [119]. Polymeric nanocomposites (composites in which at least one of the phases shows dimensions in the nanometer range) using nanocellulose have been of increasing interest due to their unique characteristics, such as high strength, (potentially) low cost, and renewability [120].

The main processing methods used to obtain CNC-based nanocomposites are Solvent Casting, Melt Blending, and In-situ Polymerization. Each of these methods has some advantages and disadvantages. The Solvent Casting method is easy to prepare and there is the possibility of forming a three-dimensional CNC network within the polymer matrix. Nonetheless, this method makes use of generally hazardous solvents (environmental issues) and therefore they are produced on a small scale. The Fusion Mixing method has great potential for large-scale mass production, in which the use of hazardous solvents is not necessary. However, CNCs can degrade during the process and high shear applied during the process does not allow the formation of the three-dimensional CNC network. Finally, the in-situ polymerization method allows the formation of a polymeric network with relatively uniformly embedded CNCs and with the covalent bond between CNCs and the polymer matrix having the potential for large-scale production. But the polymerization temperature in this method can degrade the CNCs during the process and the dispersion of the CNCs in the monomeric phase can lead to a low degree of polymerization [121].

Nanocellulose has also gained much research attention as a filler application due to its biodegradability. These nanocellulose-based polymers have the advantage of being biodegradable but are based on matrix and reinforcement in the polymers. Nanocellulose is actively used in the preparation of polymers, films, nanocomposites, hydrogels, and various other prospects [122]. Besides contributing to improving the stability and strength of the films, the addition of CNC promotes the biodegradation process, since CNC has a high surface area, increasing exposure to microorganisms in the soil and improving the rate of degradation. Thus, the higher the proportion of CNC in polymer films, the higher the degradation rate together with greater weight loss [123].

PLA/CNC Nanocomposites

Nanocellulose has low compatibility with a hydrophobic polymer like PLA. To overcome this problem, it is necessary to introduce a plasticizer [124]. Asraf et al. [125] used various proportions of epoxidized palm oil (EPO) as a plasticizer in PLA and nanocrystalline cellulose blends. In which the mechanical properties were improved and the rate of soil degradation was increased as the plasticizer amount increased. As the proportion of CNC in PLA increases, the flow resistance decreases. Therefore, with an increase in wt% CNC Young's Modulus increases, indicating that the addition of CNC has good adhesion to the PLA matrix. The elongation at break for the CNC composite with 10% by weight of EPO is the highest (213%), which indicates that the ductility of the composite is increased. However, the elongation at break of nanocomposite starts to decrease with EPO at 15% by weight, due to the accumulation of excess EPO in the interfacial area of the material.

In the study of Faraj et al. [126], they analyzed two types of surface compatibilizer (fatty acids and PGMA with reactive end-groups) in nanocomposites of PLA and surface-grafted CNC with concentrations up to 50 wt% CNC particles. The CNC-g-PGMA epoxy groups reacted with each other and with the PLA, forming a phase separation system. This system did not percolate, and its mechanical performance was governed by the covalent filler/matrix coupling. However, the fatty acids were efficient CNC dispersants in the matrix and the gain in the rubbery elastic modulus was very important. This can be attributed to percolation, although the strength of the percolated network was transmitted by the surface graft because it prevented the establishment of inter–CNC H-bonds. Therefore, in this case, the system that uses fatty acids and a very simple and scalable surface grafting method was the most efficient.

And Mujica-Garcia et al. [127] analyzed the compatibilization of PLA/CNC with 1 wt% of CNC using PLLA chains grafted onto the CNC surface using a "grafting from" reaction. The results show that mechanical properties of the PLA nanocomposite fibers were significantly improved with the addition of only 1 wt% of CNC, with and without the compatibilizer agent. However, PLLA-grafted nanocrystals (CNC-g-PLLA) resulted in higher stress and toughness. These results showed better interfacial adhesion between CNC-g-PLLA and the PLA matrix, indicating that the grafting is affecting positively the properties acting as a flexible interface between the nanocellulose and the PLA, leading to a greater degree of alignment of the molecular chains of the CNC and the polymer.

Many studies analyze changes in mechanical properties when adding CNC to PLA. Table 7 summarizes some literature reports of tensile strength, tensile modulus and elongation at break characteristics in neat PLA and in the PLA/CNC nanocomposites. Through these studies it was observed that the addition of small amounts of CNC can generate an increase in the tensile strength of the nanocomposite, but as this proportion increases, there is a tendency towards a reduction in tensile strength. The tensile modulus of PLA shows a tendency to increase when CNC is added to its composition. On the other hand, as expected,

Table 7 Mechanical properties of PLA and PLA/CNC

CNC content (wt%)	Preparation procedure	Tensile strength (MPa)		Tensile modulus (GPa)		Elongation at break (%)		References
		PLA	PLA/CNC	PLA	PLA/CNC	PLA	PLA/CNC	
1	Solvent casting + Melting mixing	48.08 ± 1.62	48.82 ± 2.65	2.188 ± 0.348	2.425 ± 0.168	4.04 ± 0.77	3.45 ± 0.14	[210]
3	Solvent casting + Melting mixing	48.08 ± 1.62	47.83 ± 0.59	2.188 ± 0.348	2.240 ± 0.069	4.04 ± 0.77	2.86 ± 0.32	[210]
5	Solvent casting + Melting mixing	48.08 ± 1.62	46.07 ± 1.30	2.188 ± 0.348	2.331 ± 0.270	4.04 ± 0.77	3.56 ± 0.28	[210]
1	Extrusion + compression molding	54.6 ± 0.3	56.2 ± 0.9	1.166 ± 0.055	1.343 ± 0.041	6.3 ± 0.4	6.4 ± 0.4	[211]
3	Extrusion + compression molding	54.6 ± 0.3	59.9 ± 2.4	1.166 ± 0.055	1.419 ± 0.029	6.3 ± 0.4	5.5 ± 0.5	[211]
5	Extrusion + compression molding	54.6 ± 0.3	54.9 ± 0.8	1.166 ± 0.055	1.442 ± 0.027	6.3 ± 0.4	4.9 ± 0.1	[211]
1	Solvent casting	52.3 ± 0.02	72.9 ± 0.05	1.95 ± 0.05	2.12 ± 0.07	3.86 ± 0.13	4.02 ± 0.12	[212]
2	Solvent casting	52.3 ± 0.02	68.6 ± 0.06	1.95 ± 0.05	2.05 ± 0.03	3.86 ± 0.13	3.51 ± 0.10	[212]
3	Solvent casting	52.3 ± 0.02	65.5 ± 0.06	1.95 ± 0.05	1.92 ± 0.03	3.86 ± 0.13	3.54 ± 0.13	[212]
0.5	Solvent casting[a]	47.9 ± 4.6	52.0 ± 2.2	1.61 ± 0.16	1.66 ± 0.16	3.4 ± 0.4	4.3 ± 0.8	[213]
1	Solvent casting[a]	47.9 ± 4.6	45.3 ± 2.3	1.61 ± 0.16	1.82 ± 0.16	3.4 ± 0.4	12.3 ± 4.6	[213]
3	Solvent casting[a]	47.9 ± 4.6	40.2 ± 1.2	1.61 ± 0.16	1.72 ± 0.14	3.4 ± 0.4	8.3 ± 2.5	[213]

[a]using poly(vinyl alcohol) (PVA) solvent in CNCs solution and polyethylene glycol (PEG) as plasticizer; "- " Unknown

the elongation values at break of PLA were, in most cases, reduced with CNC loading.

In the study of Zaaba et al. [128], they investigated two types of nanocellulose (CNC and CNF) used in PLA bionanocomposites. The addition of CNC generated brittle PLA nanocomposites. But in addition, this can be solved by performing a pre-treatment on nanocellulose particles to increase the interfacial interaction between the bionanocomposites elements. The incorporation of CNF reduced elongation at break, improved tensile strength, and modulus of PLA composites.

The method of preparation of PLA/CNC is an aspect that can influence the properties of the nanocomposites. In the work of Bagheriasl et al. [129], the efficiency PLA/CNC nanocomposites preparation was compared by two different methods, via a solution-cast method and further diluted with neat PLA in the melt state using either a twin-screw extruder or an internal batch mixer, and via direct melt mixing method. When the solution-prepared PLA/CNC masterbatch was used to develop the nanocomposites via extrusion and internal batch mixing occured a good dispersion of the hydrophilic CNCs within the PLA matrix and led to the formation of a network of CNCs. Consequently, improved the thermal and mechanical properties of the PLA, in constrast to the cases of neat PLA and PLA/CNC prepared by direct melt blending. Therefore, the most efficient method for preparing PLA/CNC nanocomposites in was the use of solution-based in PLA/CNC masterbatch, followed by melt extrusion of the masterbatch and PLA.

By the other way, the study of Arslan et al. [130], PLA/CNC nanocomposites were prepared via solution casting and via dilution of solution-casted PLA/CNC masterbatch though melt mixing in a twin screw extruder. CNC nanoparticles revealed a better dispersion quality in the samples prepared through the casting solution, whereas the formation of CNC agglomerates was observed in the melt-processed nanocomposites. And CNC incorporation promoted heterogeneous crystal nucleation in PLA/CNC nanocomposites prepared by masterbatch though melt mixing during cooling, whereas in solution casting samples, crystal nucleation was observed to be more dominant in the first scan of heating.

Numerous studies are carried out to indicate the biodegradability of such polymers. For instance, Asraf et al. [125] evaluated the effects of the altered ratios of CNC and plasticizer (EPO) in PLA on soil burial tests. And it was observed that the degradation rate of the PLA/EPO/CNC in the soil, in 6th month, increased with the increasing of the CNC weight% (by 11.29%, 12.04% and 12.30% for PLA/EPO5% with CNC5%, CNC10%, and CNC15%, respectively) but increased even more with a higher % by weight of EPO (at 13.06% and 15.37% for PLA/CNC5% with EPO10% and EPO15%, respectively).

Sucinda et al. [123] analyzed the soil burial biodegradability of neat PLA and PLA/CNC, in which neat PLA degraded slowly in the soil, with a total weight loss of only 3.93% at day 75. In contrast, the nanocomposite samples PLA/CNC achieved greater weight loss at 75 days, whereas the CNC content increased, and the degradation rate of the PLA/CNC films improved. For PLA with the addition of 0.5, 1.0, 1.5, 2.0 and 3.0% of CNC, the total weight loss was observed to be 4.30%, 6.57%, 6.78%, 7.30% and 7.57%, respectively.

Wang et al. [131] evaluated the weight loss in hydrolytic and soil degradation of PLA with the addition of 0 to 15 wt% of crystalline nanocellulose with zinc oxide (CNC–ZnO)

hybrids as green nanofillers. The neat PLA and PLA nanocomposite films were incubated for 70 days under composting conditions in phosphate buffered saline (PBS) and in soil burial for 110 days. For the hydrolytic degradation, the more CNC–ZnO hybrids were added the faster degradation rate was obtained. After 70 days of exposure, the weight loss of neat PLA reached only 9%, while for PLA nanocomposite film with 15 wt% CNC–ZnO hybrids reached 25% of weight loss. For the soil burial degradation, neat PLA showed the smallest degradation rate, 8% weight loss after 110 days, while by adding 15 wt% CNC-ZnO hybrids, the PLA nanocomposite film degraded about 28% after 110 days, therefore it can be fully degraded within 1 year. It was also observed that due to the hydrophobic nature of PLA, it is difficult for water to pass into the films, but due excellent hydrophilicity and water solubility of CNC, PLA/CNC nanocomposites could benefit absorbs and maintain the water.

PBAT/CNC Nanocomposites

A few studies report the properties of PBAT/CNC nanocomposites. Bauli et al. [132] studied nanocellulose crystalline, obtained by enzymatic hydrolysis, incorporated into the PBAT matrix (at 1%, 3%, and 5% by weight) by a solvent casting method. Nanocellulose composites with and without alkaline pretreatment for lignin removal, called P and N, respectively, were prepared. The mechanical properties of PBAT nanocomposites with 1%P and 1%N showed improvement of 12% and 11% in Young's modulus, respectively. The tensile strength in 1%P increased by 12% but in 1%N was maintained, considering the error, compared with the neat matrix. The degradation analysis in simulated soil showed that both material with P and N showed degradation rates like those of neat PBAT. Therefore, according to the properties analyzed, the pre-treatment process was not considered necessary, as the results for P and N were similar.

This behavior of improving the mechanical properties and not changing the biodegradation of the nanocomposite was also observed in Morelli et al. [133], PBAT nanocomposites with cellulose nanocrystals with 2.5, 5, and 10 wt% of CNC chemically modified with phenylbutyl isocyanate was analyzed. This modification aims to avoid CNC aggregation during the drying and extrusion process. PBAT is very ductile and after the incorporation of the CNC, its ductility has not changed. The samples with CNC also had an elastic modulus considerably higher than the values of the neat PBAT, and higher CNC contents led to higher increases. The addition of non-modified and modified CNC increased the modulus of elasticity of the PBAT for about 55% and 39%, respectively, in the 10 wt% nanocomposites. The chemical modification of the CNC increased its thermal stability and reduced the water vapor permeability of PBAT, and this decrease was greater in the modified CNC-based nanocomposites (approximately 63%). However, the incorporation of CNC did not compromise the biodegradation of PBAT, even after its chemical modification.

Different methods of preparation were evaluated in the study of Vatansever et al. [134], in which they evaluated two different preparation methods for PBAT/CNC nanocomposites, the solution casting (SC) and dilution of the solution-casted masterbatch through TSE (mTSE) preparation methods. The neat PBAT and PBAT/CNC with 1, 3, and 5 wt% of CNC for both preparation methods were analyzed. It was reported that the tensile strength of PBAT was increased upon the addition of 1 wt% CNC for both preparation methods. However, the increase of CNC content led to a decrease in tensile strength of the nanocomposites. The tensile modulus of PBAT was not affected with 1 w% of CNC but at 5wt% CNC the nanocomposites showed higher elastic modulus because of a better CNC dispersion. On the other hand, the elongation at break values of PBAT was lowered with the CNC loading regardless of preparation method.

Also considering the work of Zhang et al. [135], nanocomposites of PBAT with cellulose nanocrystals (PBAT/CNC) and with acetylated CNC modified by acetic anhydride (PBAT/ACNC) were evaluated. After the modification of acetic anhydride, the hydrophilicity of CNC decreased and the dispersion of CNC in PBAT was improved. PBAT/ACNC nanocomposites had better mechanical properties, thermal stability and glass transition temperature than PBAT/CNC, however, the biodegradable properties do not appear to change with the addition of ACNC in the PBAT.

PLA/PBAT/CNC Nanocomposites

As shown by some studies, the addition of nanocellulose in the PLA/PBAT blend can impose variable mechanical properties according to the phase in which the nanocellulose is added (either in the PLA matrix phase, in the PBAT dispersed phase, or in both phases) and the type of processing of the material [26, 27, 31, 136].

In the work of Mohammadi et al. [27], mechanical properties of PLA/PBAT (75 wt%/25 wt%) blends, alternating with semicrystalline PLA (scPLA) and amorphous PLA (aPLA), and with the addition of 1 wt% of CNCs was investigated. The CNCs were incorporated in the matrix phase (PLA) and in both phases (matrix phase—PLA and dispersed phase—PBAT). In both interface localizations, considerable improvements in elongation at break and impact properties of scPLA/PBAT were observed with the addition of 1 wt% CNCs. These improvements were less effective in the case of PLA/PBAT/CNC due to the higher residual solvent in this system and the better affinity of CNCs with the solvent.

Considering the work of Mohammadi et al. [26], they also analyzed PLA/PBAT (75 wt%/25 wt%) blends, alternating with semicrystalline PLA (scPLA) and amorphous PLA (aPLA), and with the addition of 1 wt% of CNCs incorporated in the matrix phase and in both phases, but focusing in rheological and morphological properties. Mostly, the incorporation of CNCs shown to decrease the PBAT droplet size and create a finer morphology in the blended nanocomposites, but when the CNCs were initially dispersed in the PLA and in both phases, they tended to be located at the interface of the PLA and PBAT phases, favoring the stabilization of the blend morphology under shear flow. The introduction of 1 wt% of CNC in PLA and in both phases delayed the relaxation of the drops due to the formation of the network of CNCs.

Hosseinnezhad et al. [136] investigated the mechanical properties of PLA/PBAT (90/10 wt%) blends and composites with 3% and 7% of CNFs in both phases. The introduction of CNFs showed an increase in modulus of elasticity, yield stress, and tensile strength in both blends and nanocomposites. However, unlike the highly embrittled PLA/PBAT/CNFs blends, PLA/PBAT/CNFs nanocomposites retain a sufficiently high degree of plasticity. Then, in situ generated products can be considered effective polymer materials with triple shape memory.

The methods used for the preparation and processing can also affect the final properties of the PLA/PBAT/CNC nanocomposites. In Sarul et al. [31], mechanical properties of PLA/PBAT (75 wt%/25 wt%) blends with 3 wt % of CNC were analyzed with different processing techniques (by a corotating twin-screw extruder (TSE) and by an internal mixer (IM)) and different localization of CNCs (matrix phase—PLA, dispersed phase—PBAT, and in both phases). It was found that the tensile strength of the blend prepared with IM was lower than that prepared with TSE. The tensile modulus of PLA/PBAT blends with 3 wt% of CNC, was higher than the neat PLA only for the blend with CNC localization in PBAT phase ((PBAT/CNC)/PLA) and prepared with IM. Also, higher elongation at break was found for this formulation but prepared with TSE instead. Izod impact tests revealed that the toughness decreased in the blend containing 3 wt% of CNC prepared with TSE and increase prepared with the IM compared to the neat blend. Therefore, solvent preparation methods can make the samples quite brittle in as much as that compression molding is not possible, and the expected enhancement in the impact strength, ductility, and toughness was not attained despite significant rheological improvements obtained.

Also, in Sarul et al. [30], the effect of CNC on the properties of PLA/PBAT blends was investigated and prepared by two methods, solution casting (SC), and a combination of solution casting and melt mixing through twin-screw extruder (mTSE). For the samples prepared via SC, the rheological experiments, with the addition of 3% by weight of CNC, shown a large increase in complex viscosity and in the storage modulus at low frequencies, which was pointed that this can be attributed to the formation of the CNC network in the PLA matrix. With the increase to 5 wt% of CNC this was more evidenced. And for the samples prepared via mTSE, no significant increase in the rheological properties was observed, because the reagglomeration of CNCs could suppress the melting properties of the nanocomposites. The mechanical properties of neat PLA, PLA/PBAT blend, and PLA/PBAT/CNC nanocomposites prepared by mTSE are illustrated in Fig. 6. Comparing the PLA/PBAT blend with the PLA/PBAT/CNC nanocomposites, it is possible to observe a improvement in tensile strength as the CNC content increases, a increase in Young's modulus for PLA/PBAT containing 5 wt% of CNC, but as the CNC content increases, the elongation at break decreases, and for the energy at break, a reduction in the nanocomposites compared to the blend is shown.

CNC is more dispersed in the PLA phase than in the PBAT phase, because when CNCs are introduced into the blend through the PBAT phase, they remain in the PBAT droplets reducing their droplet size, while when added in the PLA matrix phase or in both phases, it results in elongated PBAT droplets with a tendency for the PLA matrix to show a co-continuous morphology [27, 31].

Efforts were concentrated to understand the contribution of the degradation promoted by radiation in the nanocomposites [137, 138]. However, the evaluation of the biodegradability of the PLA/PBAT blend reinforced with nanocellulose is still a poorly studied field in the literature, other than, the effects of radiation on the nanocellulose in polymer blends.

Andrade et al. [139] analyzed nanocomposite films of PLA/PBAT blends containing different amounts of crystalline nanocellulose (CNCs, 0–2% by weight), extracted from agricultural residues using a twin screw extruder and blown extrusion process. The PLA/PBAT/CNC nanocomposites showed better hydrophobic character and thermal stability than the PLA/PBAT blend. Furthermore, the tensile strength, elongation at break and Young's modulus for the nanocomposites were about 52%, 29% and 118%, respectively, higher than the blended films.

Conclusion

PLA is a very attractive biopolymer due to its characteristics of rigidity and tensile strength. To improve the ductility of PLA, its combination with PBAT has been considered. PBAT films take longer to degrade than PLA films, and besides that, when blended the biodegradation rates of PLA/PBAT are lower than those for the neat PLA and neat PBAT.

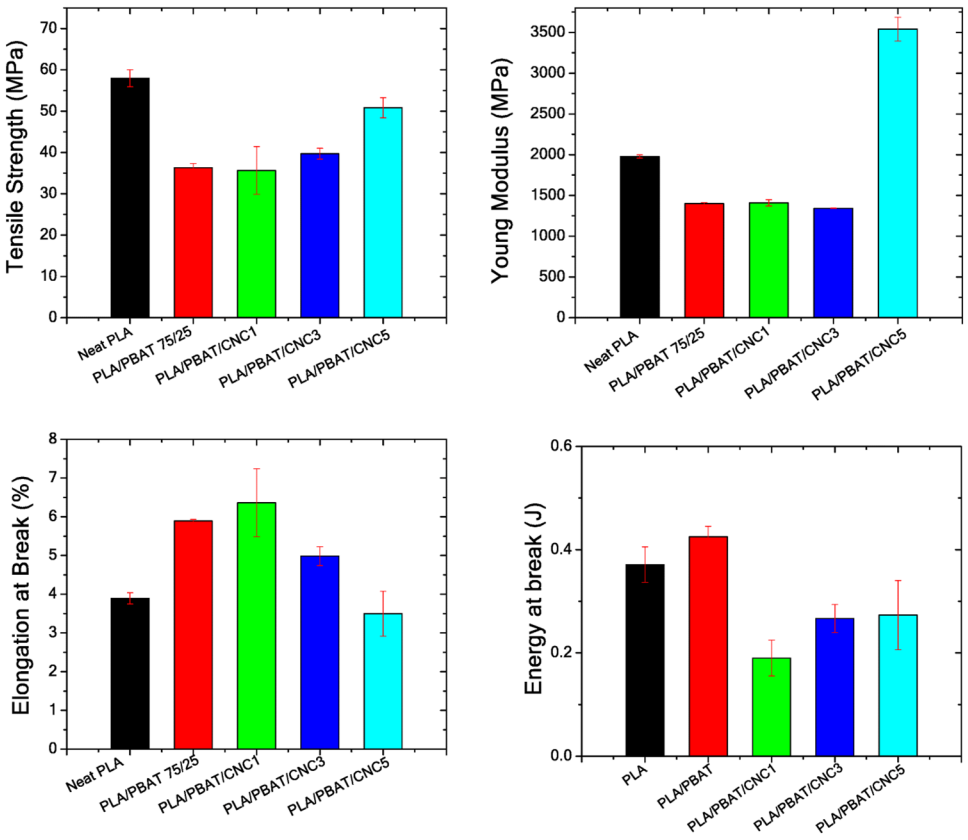

Fig. 6 Tensile properties of the neat PLA, PLA/PBAT blend, and PLA/PBAT/CNC nanocomposites with 1, 3, and 5 wt% of CNC content prepared via mTSE. (Reprinted with permission from SpringerNature) [30]

The PLA/PBAT blends, despite having low compatibility, have been widely studied as an alternative to the use of conventional petroleum-based plastics for packaging applications. In most cases, the compatibilization of multiphase polymers is through the addition of chemical compatibilizing agents, which leads to an increase in tensile strength, elongation at break, and impact strength of the PLA/PBAT blend. Although exposure to high energy radiation (such as gamma rays and electron beams) is a method that has been studied as an alternative to enhance the compatibility of multiphase polymers, there are however few studies that report the behavior of compatibilization by high energy radiation in PLA/PBAT blends. But studies with other polymers have shown an improvement in the interfacial adhesion of the blend, proving the efficiency of this method in the compatibilization of immiscible blends.

Nanocrystalline cellulose (CNCs) has been widely studied as a reinforcement phase in biodegradable polymers due to its biodegradability, wide availability in nature, and ability to improve the properties of composites. The polymer properties can be improved with the addition of CNC, but this can vary according to the fiber source, the extraction, and processing method, concentration, and the phase in which it is added to the polymer composite. Both CNCs and CNFs enhance the mechanical properties of the PLA/PBAT blend, and the properties may vary with the phase in which the nanocellulose is being inserted, the type of fiber treatment, the proportion of fiber in the blend and the preparation methodology. Nevertheless, few studies evaluate the behavior of the addition of crystalline nanocellulose in the PLA/PBAT blend, much less the compatibilization of this biocomposite by ionizing radiation.

PLA films are more transparent than PBAT films, and the color of PLA/PBAT composite films became more off-white with the increase of PBAT content. The addition of nanocellulose in PLA, PBAT, and in the PLA/PBAT blend shows an increase in the opacity of the films, but there are still no studies that report whether the immiscible blends are opaque and become transparent after compatibilization.

Studies of blends and nanocomposites of biodegradable polymers have been focused on the search for reinforcing agents and suitable processes that promote the physical and mechanical properties with the protection of the relative integrity of the components in conditions of compatibility, and adhesion at the level of the polymer-nanofiber interfaces. In this sense, the development of such materials is still on the way to investigating the use of radiation or chemical modification as a compatibilizer promoter for blending, and surface modifier of cellulosic nanoparticles for superior filler dispersion and interfacial mechanical resistance to assure the better properties of such a short time shelf-life of the biodegradable products derived from PLA/PBAT.

Acknowledgements To the support of CNPq and IPEN/CNEN.

Author Contributions FATdC: data curation, writing-original draft preparation. DFP: writing- reviewing and editing, validation. ECLC: writing- reviewing and editing. OG: reviewing and editing.

Funding No funding was received to assist with the preparation of this manuscript.

Declarations

Conflict of interest The authors have no competing interests to declare that are relevant to the content of this manuscript.

References

1. Chen Y, Geever LM, Killion JA, Lyons JG, Higginbotham CL, Devine DM (2016) Review of multifarious applications of poly (Lactic Acid). Polym-Plast Technol Eng 55(10):1057–1075. https://doi.org/10.1080/03602559.2015.1132465
2. Garlotta D (2019) A literature review of Poly (Lactic Acid) a literature review of Poly (Lactic Acid). J Polym Environ 9(2):63–84. https://doi.org/10.1023/A:1020200822435
3. Saini P, Arora M, Kumar MNVR (2016) Poly(lactic acid) blends in biomedical applications. Adv Drug Deliv Rev 107:47–59. https://doi.org/10.1016/j.addr.2016.06.014
4. Sinclair RG (1996) The case for polylactic acid as a commodity packaging plastic. J Macromol Sci, Part A 33(5):585–597. https://doi.org/10.1080/10601329608010880
5. Södergård A, Stolt M (2002) Properties of lactic acid based polymers and their correlation with composition. Prog Polym Sci 27(6):1123–1163. https://doi.org/10.1016/S0079-6700(02)00012-6
6. Zhao X, Hu H, Wang X, Yu X, Zhou W, Peng S (2020) Super tough poly(lactic acid) blends: a comprehensive review. RSC Adv 10(22):13316–13368. https://doi.org/10.1039/D0RA01801E
7. Ouchi T, Ohya Y (2004) Design of lactide copolymers as biomaterials. J Polym Sci, Part A: Polym Chem 42(3):453–462. https://doi.org/10.1002/pola.10848
8. Zhang T, Han W, Zhang C, Weng Y (2021) Effect of chain extender and light stabilizer on the weathering resistance of PBAT/PLA blend films prepared by extrusion blowing. Polym Degrad Stab 183:109455. https://doi.org/10.1016/j.polymdegradstab.2020.109455
9. de Castro JG, Rodrigues BVM, Ricci R, Costa MM, Ribeiro AFC, Marciano FR, Lobo AO (2016) Designing a novel nanocomposite for bone tissue engineering using electrospun conductive PBAT/polypyrrole as a scaffold to direct nanohydroxyapatite electrodeposition. RSC Adv 6(39):32615–32623. https://doi.org/10.1039/C6RA00889E
10. Gross RA, Kalra B (2002) Biodegradable polymers for the environment. Science 297(5582):803–807. https://doi.org/10.1126/science.297.5582.803
11. Jian J, Xiangbin Z, Xianbo H (2020) An overview on synthesis, properties and applications of poly(butylene-adipate-co-terephthalate)–PBAT. Adv Ind Eng Polym Res 3(1):19–26. https://doi.org/10.1016/j.aiepr.2020.01.001
12. Kijchavengkul T, Auras R, Rubino M, Selke S, Ngouajio M, Fernandez RT (2010) Biodegradation and hydrolysis rate of aliphatic aromatic polyester. Polym Degrad Stab 95(12):2641–2647. https://doi.org/10.1016/j.polymdegradstab.2010.07.018
13. Pereira da Silva JS, Farias da Silva JM, Soares BG, Livi S (2017) Fully biodegradable composites based on poly(butylene adipate-co-terephthalate)/peach palm trees fiber. Compos B Eng 129:117–123. https://doi.org/10.1016/j.compositesb.2017.07.088
14. Rodrigues BVM, Silva AS, Melo GFS, Vasconscellos LMR, Marciano FR, Lobo AO (2016) Influence of low contents of superhydrophilic MWCNT on the properties and cell viability of electrospun poly (butylene adipate-co-terephthalate) fibers. Mater Sci Eng, C 59:782–791. https://doi.org/10.1016/j.msec.2015.10.075
15. Santana-Melo GF, Rodrigues BVM, da Silva E, Ricci R, Marciano FR, Webster TJ, Vasconcellos LMR, Lobo AO (2017) Electrospun ultrathin PBAT/nHAp fibers influenced the in vitro and in vivo osteogenesis and improved the mechanical properties of neoformed bone. Colloids Surf, B 155:544–552. https://doi.org/10.1016/j.colsurfb.2017.04.053
16. van de Velde K, Kiekens P (2002) Biopolymers: overview of several properties and consequences on their applications. Polym Testing 21(4):433–442. https://doi.org/10.1016/S0142-9418(01)00107-6
17. Al-Itry R, Lamnawar K, Maazouz A (2014) Rheological, morphological, and interfacial properties of compatibilized PLA/PBAT blends. Rheol Acta 53(7):501–517. https://doi.org/10.1007/s00397-014-0774-2
18. Ding Y, Lu B, Wang P, Wang G, Ji J (2018) PLA-PBAT-PLA tri-block copolymers: Effective compatibilizers for promotion of the mechanical and rheological properties of PLA/PBAT blends. Polym Degrad Stab 147:41–48. https://doi.org/10.1016/j.polymdegradstab.2017.11.012
19. Kim T-J, Kim T-H, Kim S-G, Seo K-H (2016) Structural, thermal, and mechanical properties of PLA/PBAT/MEA blend. Polym Korea 40(3):371. https://doi.org/10.7317/pk.2016.40.3.371
20. Moustafa H, el Kissi N, Abou-Kandil AI, Abdel-Aziz MS, Dufresne A (2017) PLA/PBAT bionanocomposites with antimicrobial natural rosin for green packaging. ACS Appl Mater Interfaces 9(23):20132–20141. https://doi.org/10.1021/acsami.7b05557
21. Sun Z, Zhang B, Bian X, Feng L, Zhang H, Duan R, Sun J, Pang X, Chen W, Chen X (2015) Synergistic effect of PLA–PBAT–PLA tri-block copolymers with two molecular weights as compatibilizers on the mechanical and rheological properties of PLA/PBAT blends. RSC Adv 5(90):73842–73849. https://doi.org/10.1039/C5RA11019J
22. Mostafapoor F, Khosravi A, Fereidoon A, Khalili R, Jafari SH, Vahabi H, Formela K, Saeb MR (2020) Interface analysis of compatibilized polymer blends. in compatibilization of polymer blends. Elsevier, Netherlands, pp 349–371
23. Spontak RJ, Ryan JJ (2020) Polymer blend compatibilization by the addition of block copolymers. Compatibilization of polymer blends. Elsevier, Netherlands, pp 57–102
24. Fu Y, Wu G, Bian X, Zeng J, Weng Y (2020) Biodegradation behavior of Poly(Butylene Adipate-Co-Terephthalate) (PBAT), Poly(Lactic Acid) (PLA), and their blend in freshwater with sediment. Molecules 25(17):3946. https://doi.org/10.3390/molecules25173946
25. Subramanian MN (2017) Polymer blends and composites. in springer series in surface sciences. John Wiley & Sons, Inc, Hoboken, p 52
26. Mohammadi M, Heuzey M-C, Carreau PJ, Taguet A (2021) Morphological and rheological properties of PLA, PBAT, and PLA/PBAT blend nanocomposites containing CNCs. Nanomaterials 11(4):857. https://doi.org/10.3390/nano11040857
27. Mohammadi M, Heuzey M-C, Carreau PJ, Taguet A (2021) Interfacial localization of CNCs in PLA/PBAT blends and its effect on rheological, thermal, and mechanical properties. Polymer 233:124229. https://doi.org/10.1016/j.polymer.2021.124229

28. Osman, M. J., Ibrahim, N. A., Sharif, J., & Wan Yunus, W. M. Z. (2014). Study on water absorption and biodegradation of polylactic acid / poly (butylene adipate-co-terephthalate) nanocomposite. *ChemXpress*, *5*(2), 66–72. https://www.tsijournals.com/abstract/study-on-water-absorption-and-biodegradation-of-polylactic-acidpoly-butylene-adipatecoterephthalate-nanocomposite-1615.html
29. Qiu S, Zhou Y, Waterhouse GIN, Gong R, Xie J, Zhang K, Xu J (2021) Optimizing interfacial adhesion in PBAT/PLA nanocomposite for biodegradable packaging films. Food Chem 334:127487. https://doi.org/10.1016/j.foodchem.2020.127487
30. Sarul DS, Arslan D, Vatansever E, Kahraman Y, Durmus A, Salehiyan R, Nofar M (2021) Preparation and characterization of PLA/PBAT/CNC blend nanocomposites. Colloid Polym Sci 299(6):987–998. https://doi.org/10.1007/s00396-021-04822-9
31. Sema Sarul D, Arslan D, Vatansever E, Kahraman Y, Durmus A, Salehiyan R, Nofar M (2022) Effect of mixing strategy on the structure-properties of the PLA/PBAT blends incorporated with CNC. J Renew Mater 10(1):149–164. https://doi.org/10.32604/jrm.2022.017003
32. Salzano de Luna M, Filippone G (2016) Effects of nanoparticles on the morphology of immiscible polymer blends—challenges and opportunities. Eur Polymer J 79:198–218. https://doi.org/10.1016/j.eurpolymj.2016.02.023
33. Taguet A, Cassagnau P, Lopez-Cuesta J-M (2014) Structuration, selective dispersion and compatibilizing effect of (nano)fillers in polymer blends. Prog Polym Sci 39(8):1526–1563. https://doi.org/10.1016/j.progpolymsci.2014.04.002
34. Fenouillot F, Cassagnau P, Majesté J-C (2009) Uneven distribution of nanoparticles in immiscible fluids: Morphology development in polymer blends. Polymer 50(6):1333–1350. https://doi.org/10.1016/j.polymer.2008.12.029
35. Dong X, Wu Z, Wang Y, Li T, Zhang X, Yuan H, Xia B, Ma P, Chen M, Dong W (2021) Toughening polylactide using epoxy-functionalized core-shell starch nanoparticles. Polym Test 93:106926. https://doi.org/10.1016/j.polymertesting.2020.106926
36. Morão A, de Bie F (2019) Life cycle impact assessment of polylactic acid (PLA) Produced from sugarcane in Thailand. J Polym Environ 27(11):2523–2539. https://doi.org/10.1007/s10924-019-01525-9
37. Cuiffo MA, Snyder J, Elliott AM, Romero N, Kannan S, Halada GP (2017) Impact of the fused deposition (FDM) printing process on polylactic acid (PLA) chemistry and structure. Appl Sci 7(6):579. https://doi.org/10.3390/app7060579
38. Su S, Kopitzky R, Tolga S, Kabasci S (2019) Polylactide (PLA) and Its blends with poly(butylene succinate) (PBS): a brief review. Polymers 11(7):1193. https://doi.org/10.3390/polym11071193
39. Foroughi F, Rezvani Ghomi E, Morshedi Dehaghi F, Borayek R, Ramakrishna S (2021) A review on the life cycle assessment of cellulose: from properties to the potential of making it a low carbon material. Materials 14(4):714. https://doi.org/10.3390/ma14040714
40. Su S (2021) Prediction of the miscibility of PBAT/PLA blends. Polymers 13(14):2339. https://doi.org/10.3390/polym13142339
41. Zaaba NF, Jaafar M (2020) A review on degradation mechanisms of polylactic acid: Hydrolytic, photodegradative, microbial, and enzymatic degradation. Polym Eng Sci 60(9):2061–2075. https://doi.org/10.1002/pen.25511
42. García-Masabet V, Santana Pérez O, Cailloux J, Abt T, Sánchez-Soto M, Carrasco F, Maspoch ML (2019) PLA/PA Bio-Blends: induced morphology by extrusion. Polymers 12(1):10. https://doi.org/10.3390/polym12010010
43. DeStefano V, Khan S, Tabada A (2020) Applications of PLA in modern medicine. Eng Regen 1:76–87. https://doi.org/10.1016/j.engreg.2020.08.002
44. Sharif A, Mondal S, Hoque ME (2019) Polylactic acid (PLA)-Based nanocomposites processing and properties. In: Sanyang ML, Jawaid M (eds) Bio-based polymers and nanocomposites. Springer International Publishing, Cham, pp 233–254
45. ASTM D5338-98. (2003). Standard Test Method for Determining Aerobic Biodegradation of Plastic Materials Under Controlled Composting Conditions. *ASTM International*, *98*(Reapproved), 1–6. https://doi.org/10.1520/D5338-98R03
46. ASTM D5988–12. (2012). Standard Test Method for Determining Aerobic Biodegradation of Plastic Materials in Soil. *ASTM International*, 1–6. https://doi.org/10.1520/D5988-12
47. Kalita NK, Nagar MK, Mudenur C, Kalamdhad A, Katiyar V (2019) Biodegradation of modified poly(lactic acid) based biocomposite films under thermophilic composting conditions. Polym Test 76(February):522–536. https://doi.org/10.1016/j.polymertesting.2019.02.021
48. Vasile C, Pamfil D, Râpă M, Darie-Niţă RN, Mitelut AC, Popa EE, Popescu PA, Draghici MC, Popa ME (2018) Study of the soil burial degradation of some PLA/CS biocomposites. Compos B Eng 142:251–262. https://doi.org/10.1016/j.compositesb.2018.01.026
49. Janczak K, Hrynkiewicz K, Znajewska Z, Dąbrowska G (2018) Use of rhizosphere microorganisms in the biodegradation of PLA and PET polymers in compost soil. Int Biodeterior Biodegradation 130:65–75. https://doi.org/10.1016/j.ibiod.2018.03.017
50. Qi X, Ren Y, Wang X (2017) New advances in the biodegradation of poly(lactic) acid. Int Biodeterior Biodegradation 117:215–223. https://doi.org/10.1016/j.ibiod.2017.01.010
51. Gambarini V, Pantos O, Kingsbury JM, Weaver L, Handley KM, Lear G (2021) Phylogenetic distribution of plastic-degrading microorganisms. MSystems. https://doi.org/10.1128/mSystems.01112-20
52. Richert A, Dąbrowska GB (2021) Enzymatic degradation and biofilm formation during biodegradation of polylactide and polycaprolactone polymers in various environments. Int J Biol Macromol 176:226–232. https://doi.org/10.1016/j.ijbiomac.2021.01.202
53. Pattanasuttichonlakul W, Sombatsompop N, Prapagdee B (2018) Accelerating biodegradation of PLA using microbial consortium from dairy wastewater sludge combined with PLA-degrading bacterium. Int Biodeterior Biodegradation 132(March):74–83. https://doi.org/10.1016/j.ibiod.2018.05.014
54. Ferreira FV, Cividanes LS, Gouveia RF, Lona LMF (2019) An overview on properties and applications of poly(butylene adipate- co -terephthalate)-PBAT based composites. Polym Eng Sci 59(s2):E7–E15. https://doi.org/10.1002/pen.24770
55. Soulenthone P, Tachibana Y, Muroi F, Suzuki M, Ishii N, Ohta Y, Kasuya K (2020) Characterization of a mesophilic actinobacteria that degrades poly(butylene adipate-co-terephthalate). Polym Degrad Stab 181:109335. https://doi.org/10.1016/j.polymdegradstab.2020.109335
56. Svoboda P, Dvorackova M, Svobodova D (2019) Influence of biodegradation on crystallization of poly (butylene adipate-co-terephthalate). Polym Adv Technol 30(3):552–562. https://doi.org/10.1002/pat.4491
57. Spiridon I, Anghel NC, Darie-Nita RN, Iwańczuk A, Ursu RG, Spiridon IA (2020) New composites based on starch/Ecoflex®/biomass wastes: Mechanical, thermal, morphological and antimicrobial properties. Int J Biol Macromol 156:1435–1444. https://doi.org/10.1016/j.ijbiomac.2019.11.185
58. Coiai S, di Lorenzo ML, Cinelli P, Righetti MC, Passaglia E (2021) Binary green blends of poly(lactic acid) with poly(butylene adipate-co-butylene terephthalate) and

poly(butylene succinate-co-butylene adipate) and their nanocomposites. Polymers 13(15):2489. https://doi.org/10.3390/polym13152489
59. Borowczak, M., Sobczyk, K., & Leluk, K. (2019). Unique properties of Ecoflex® electrospun structures. *E3S Web of Conferences*, *116*, 00011. https://doi.org/10.1051/e3sconf/201911600011
60. Ren Y, Hu J, Yang M, Weng Y (2019) Biodegradation behavior of poly (lactic acid) (PLA), poly (butylene adipate-Co-terephthalate) (PBAT), and their blends under digested sludge conditions. J Polym Environ 27(12):2784–2792. https://doi.org/10.1007/s10924-019-01563-3
61. Meyer-Cifuentes IE, Werner J, Jehmlich N, Will SE, Neumann-Schaal M, Öztürk B (2020) Synergistic biodegradation of aromatic-aliphatic copolyester plastic by a marine microbial consortium. Nat Commun 11(1):5790. https://doi.org/10.1038/s41467-020-19583-2
62. Kawai F, Kawabata T, Oda M (2020) Current state and perspectives related to the polyethylene terephthalate hydrolases available for biorecycling. ACS Sustain Chem Eng 8(24):8894–8908. https://doi.org/10.1021/acssuschemeng.0c01638
63. Jia H, Zhang M, Weng Y, Zhao Y, Li C, Kanwal A (2021) Degradation of poly(butylene adipate-co-terephthalate) by *Stenotrophomonas* sp. YCJ1 isolated from farmland soil. J Environ Sci 103:50–58. https://doi.org/10.1016/j.jes.2020.10.001
64. Xiang S, Feng L, Bian X, Li G, Chen X (2020) Evaluation of PLA content in PLA/PBAT blends using TGA. Polym Test 81:106211. https://doi.org/10.1016/j.polymertesting.2019.106211
65. Correa-Pacheco ZN, Black-Solís JD, Ortega-Gudiño P, Sabino-Gutiérrez MA, Benítez-Jiménez JJ, Barajas-Cervantes A, Bautista-Baños S, Hurtado-Colmenares LB (2019) Preparation and characterization of bio-based PLA/PBAT and cinnamon essential oil polymer fibers and life-cycle assessment from hydrolytic degradation. Polymers 12(1):38. https://doi.org/10.3390/polym12010038
66. Li W, Sun C, Li C, Xu Y, Tan H, Zhang Y (2021) Preparation of effective ultraviolet shielding poly (lactic acid)/poly (butylene adipate-co-terephthalate) degradable composite film using co-precipitation and hot-pressing method. Int J Biol Macromol 191(August):540–547. https://doi.org/10.1016/j.ijbiomac.2021.09.097
67. Wang X, Peng S, Chen H, Yu X, Zhao X (2019) Mechanical properties, rheological behaviors, and phase morphologies of high-toughness PLA/PBAT blends by in-situ reactive compatibilization. Compos Part B: Eng 173:107028. https://doi.org/10.1016/j.compositesb.2019.107028
68. Cardoso ECL, Parra DF, Scagliusi SR, Sales RM, Caviquioli F, Lugao AB (2019) Study of Bio-Based Foams Prepared from PBAT/PLA Reinforced with Bio-Calcium Carbonate and Compatibilized with Gamma Radiation. In: Almayah BA (ed) Use of Gamma Radiation Techniques in Peaceful Applications. IntechOpen, London, pp 139–156
69. Han Y, Shi J, Mao L, Wang Z, Zhang L (2020) Improvement of compatibility and mechanical performances of PLA/PBAT composites with epoxidized soybean oil as compatibilizer. Ind Eng Chem Res 59(50):21779–21790. https://doi.org/10.1021/acs.iecr.0c04285
70. Nakayama D, Wu F, Mohanty AK, Hirai S, Misra M (2018) Biodegradable composites developed from PBAT/PLA Binary blends and silk powder: compatibilization and performance evaluation. ACS Omega 3(10):12412–12421. https://doi.org/10.1021/acsomega.8b00823
71. Kahraman Y, Özdemir B, Kılıç V, Goksu YA, Nofar M (2021) Super toughened and highly ductile PLA/TPU blend systems by in situ reactive interfacial compatibilization using multifunctional epoxy-based chain extender. J Appl Polym Sci 138(20):50457. https://doi.org/10.1002/app.50457
72. Standau T, Nofar M, Dörr D, Ruckdäschel H, Altstädt V (2022) A review on multifunctional epoxy-based Joncryl® ADR chain extended thermoplastics. Polym Rev 62(2):296–350. https://doi.org/10.1080/15583724.2021.1918710
73. Wang W, Zhang X, Mao Z, Zhao W (2019) Effects of gamma radiation on the impact strength of polypropylene (PP)/high density polyethylene (HDPE) blends. Res Phys 12:2169–2174. https://doi.org/10.1016/j.rinp.2019.02.020
74. Yin Y, Deng P, Zhang W, Xing Y (2018) Effect of enhanced γ-irradiation on the compatibility of polyethylene terephthalate-based basalt fiber-reinforced composites. Adv Polym Technol 37(8):3376–3383. https://doi.org/10.1002/adv.22121
75. Aldas M, Ferri JM, Motoc DL, Peponi L, Arrieta MP, López-Martínez J (2021) Gum rosin as a size control agent of poly(Butylene Adipate-Co-Terephthalate) (PBAT) Domains to increase the toughness of packaging formulations based on polylactic acid (PLA). Polymers 13(12):1913. https://doi.org/10.3390/polym13121913
76. Zhang M, Jia H, Weng Y, Li C (2019) Biodegradable PLA/PBAT mulch on microbial community structure in different soils. Int Biodeterioration Biodegradation 145:104817. https://doi.org/10.1016/j.ibiod.2019.104817
77. Jia H, Zhang M, Weng Y, Li C (2021) Degradation of polylactic acid/polybutylene adipate-co-terephthalate by coculture of Pseudomonas mendocina and Actinomucor elegans. J Hazard Mater 403:123679. https://doi.org/10.1016/j.jhazmat.2020.123679
78. Inga-Lafebre J, Pulido-González H, González-Núñez R, Hernández-Hernández ME, Rabelero-Velasco M, Aranda-García FJ, Jasso-Gastinel CF (2019) The multirole of modified natural gums for multicomponent polymers: as coupling agents for polymers reinforced with cellulosic fibers or compatibilizers for biodegradable polymer bleNDS. Quim Nova 42(3):296–304. https://doi.org/10.21577/0100-4042.20170333
79. Harada J, de Souza AG, de Macedo JRN, Rosa DS (2019) Soil culture: influence of different natural fillers incorporated in biodegradable mulching film. J Mol Liq 273:33–36. https://doi.org/10.1016/j.molliq.2018.09.109
80. Weng Y, Jin Y, Meng Q, Wang L, Zhang M, Wang Y-Z (2013) Biodegradation behavior of poly(butylene adipate-co-terephthalate) (PBAT), poly(lactic acid) (PLA), and their blend under soil conditions. Polym Test 32(5):918–926. https://doi.org/10.1016/j.polymertesting.2013.05.001
81. Palsikowski PA, Kuchnier CN, Pinheiro IF, Morales AR (2018) Biodegradation in soil of PLA/PBAT blends compatibilized with chain extender. J Polym Environ 26(1):330–341. https://doi.org/10.1007/s10924-017-0951-3
82. Lyu Y, Chen Y, Lin Z, Zhang J, Shi X (2020) Manipulating phase structure of biodegradable PLA/PBAT system: Effects on dynamic rheological responses and 3D printing. Compos Sci Technol 200:108399. https://doi.org/10.1016/j.compscitech.2020.108399
83. Mhd Ramle SF, Ahmad NA, Mohammad Rawi NF, Zahidan NS, Geng BJ (2020) Physical properties and soil degradation of PLA/PBAT blends film reinforced with bamboo cellulose. IOP Conf Series: Earth Environ Sci 596(1):012021. https://doi.org/10.1088/1755-1315/596/1/012021
84. Phetwarotai W, Zawong M, Phusunti N, Aht-Ong D (2021) Toughening and thermal characteristics of plasticized polylactide and poly(butylene adipate-co-terephthalate) blend films: Influence of compatibilization. Int J Biol Macromol 183:346–357. https://doi.org/10.1016/j.ijbiomac.2021.04.172

85. Xia X, Xu X, Lin C, Yang Y, Zeng L, Zheng Y, Wu X, Li W, Xiao L, Qian Q, Chen Q (2020) Microalgal-immobilized biocomposite scaffold fabricated by fused deposition modeling 3d printing technology for dyes removal. Mater Manuf 12:5. https://doi.org/10.30919/esmm5f706
86. Zhang R, Cai C, Liu Q, Hu S (2017) Enhancing the melt strength of poly(lactic acid) via micro-crosslinking and blending with poly(butylene adipate-co-butylene terephthalate)for the preparation of foams. J Polym Environ 25(4):1335–1341. https://doi.org/10.1007/s10924-016-0911-3
87. Choi B, Yoo S, Park S (2018) Carbon footprint of packaging films made from LDPE, PLA, and PLA/PBAT blends in South Korea. Sustainability 10(7):2369. https://doi.org/10.3390/su10072369
88. Yan D, Wang Z, Guo Z, Ma Y, Wang C, Tan H, Zhang Y (2020) Study on the properties of PLA/PBAT composite modified by nanohydroxyapatite. J Market Res 9(5):11895–11904. https://doi.org/10.1016/j.jmrt.2020.08.062
89. Hongdilokkul P, Keeratipinit K, Chawthai S, Hararak B, Seadan M, Suttiruengwong S (2015) A study on properties of PLA/PBAT from blown film process. IOP Conf Series: Mater Sci Eng 87(1):012112. https://doi.org/10.1088/1757-899X/87/1/012112
90. Pang Y, Cao Y, Zheng W, Park CB (2022) A comprehensive review of cell structure variation and general rules for polymer microcellular foams. Chem Eng J 430:132662. https://doi.org/10.1016/j.cej.2021.132662
91. Prasong W, Muanchan P, Ishigami A, Thumsorn S, Kurose T, Ito H (2020) Properties of 3D printable poly(lactic acid)/poly(butylene adipate-co-terephthalate) blends and nano talc composites. J Nanomater 2020:1–16. https://doi.org/10.1155/2020/8040517
92. Kedzior SA, Gabriel VA, Dubé MA, Cranston ED (2021) Nanocellulose in emulsions and heterogeneous water-based polymer systems: a review. Adv Mater 33(28):2002404. https://doi.org/10.1002/adma.202002404
93. Omran AAB, Mohammed AABA, Sapuan SM, Ilyas RA, Asyraf MRM, Rahimian Koloor SS, Petrů M (2021) Micro- and nanocellulose in polymer composite materials: a review. Polymers 13(2):231. https://doi.org/10.3390/polym13020231
94. Poletto M, Ornaghi H, Zattera A (2014) Native cellulose: structure characterization and thermal properties. Materials 7(9):6105–6119. https://doi.org/10.3390/ma7096105
95. Hu B, Pu H, Sun D-W (2021) Multifunctional cellulose based substrates for SERS smart sensing: Principles, applications and emerging trends for food safety detection. Trends Food Sci Technol 110:304–320. https://doi.org/10.1016/j.tifs.2021.02.005
96. Peng B, Yao Z, Wang X, Crombeen M, Sweeney DG, Tam KC (2020) Cellulose-based materials in wastewater treatment of petroleum industry. Green Energy Environ 5(1):37–49. https://doi.org/10.1016/j.gee.2019.09.003
97. Zhou Y, Zhang X, Zhang J, Cheng Y, Wu J, Yu J, Zhang J (2021) Molecular weight characterization of cellulose using ionic liquids. Polym Test 93:106985. https://doi.org/10.1016/j.polymertesting.2020.106985
98. Seddiqi H, Oliaei E, Honarkar H, Jin J, Geonzon LC, Bacabac RG, Klein-Nulend J (2021) Cellulose and its derivatives: towards biomedical applications. Cellulose 28(4):1893–1931. https://doi.org/10.1007/s10570-020-03674-w
99. Shak KPY, Pang YL, Mah SK (2018) Nanocellulose: recent advances and its prospects in environmental remediation. Beilstein J Nanotechnol 9(1):2479–2498. https://doi.org/10.3762/bjnano.9.232
100. Trache D, Tarchoun AF, Derradji M, Hamidon TS, Masruchin N, Brosse N, Hussin MH (2020) Nanocellulose: from fundamentals to advanced applications. Front Chem 8:33. https://doi.org/10.3389/fchem.2020.00392
101. Farooq A, Patoary MK, Zhang M, Mussana H, Li M, Naeem MA, Mushtaq M, Farooq A, Liu L (2020) Cellulose from sources to nanocellulose and an overview of synthesis and properties of nanocellulose/zinc oxide nanocomposite materials. Int J Biol Macromol 154:1050–1073. https://doi.org/10.1016/j.ijbiomac.2020.03.163
102. Kumar V, Pathak P, Bhardwaj NK (2020) Waste paper: an underutilized but promising source for nanocellulose mining. Waste Manage 102:281–303. https://doi.org/10.1016/j.wasman.2019.10.041
103. Tshikovhi A, Mishra SB, Mishra AK (2020) Nanocellulose-based composites for the removal of contaminants from wastewater. Int J Biol Macromol 152:616–632. https://doi.org/10.1016/j.ijbiomac.2020.02.221
104. Ravindran L, Sreekala MS, Thomas S (2019) Novel processing parameters for the extraction of cellulose nanofibres (CNF) from environmentally benign pineapple leaf fibres (PALF): structure-property relationships. Int J Biol Macromol 131:858–870. https://doi.org/10.1016/j.ijbiomac.2019.03.134
105. Tuukkanen S, Rajala S (2018) Nanocellulose as a piezoelectric material. In: Vassiliadis SG, Matsouka D (eds) Piezoelectricity—organic and inorganic materials and applications. InTech, London, p 13
106. Sun X, Mei C, French AD, Lee S, Wang Y, Wu Q (2018) Surface wetting behavior of nanocellulose-based composite films. Cellulose 25(9):5071–5087. https://doi.org/10.1007/s10570-018-1927-8
107. Bui H, Sebaibi N, Boutouil M, Levacher D (2020) Determination and review of physical and mechanical properties of raw and treated coconut fibers for their recycling in construction materials. Fibers 8(6):37. https://doi.org/10.3390/fib8060037
108. Mulenga TK, Ude AU, Vivekanandhan C (2021) Techniques for modelling and optimizing the mechanical properties of natural fiber composites: a review. Fibers 9(1):6. https://doi.org/10.3390/fib9010006
109. Graupner N, Prambauer M, Fröhlking T, Graf C, Becker JM, Meyer K, Weber DE, Weddig NB, Wunsch T, Burgstaller C, Müssig J (2019) Copy paper as a source of reinforcement for biodegradable composites—influence of fibre loading, processing method and layer arrangement—an overview. Compos Part A: Appl Sci Manuf 120:161–171. https://doi.org/10.1016/j.compositesa.2019.02.016
110. Venkatarajan S, Subbu C, Athijayamani A, Muthuraja R (2021) Mechanical properties of natural cellulose fibers reinforced polymer composites—2015–2020: a review. Mater Today: Proc 47:1017–1024. https://doi.org/10.1016/j.matpr.2021.05.547
111. Xu A, Wang Y, Gao J, Wang J (2019) Facile fabrication of a homogeneous cellulose/polylactic acid composite film with improved biocompatibility, biodegradability and mechanical properties. Green Chem 21(16):4449–4456. https://doi.org/10.1039/C9GC01918A
112. Giri J, Lach R, Grellmann W, Susan MABH, Saiter J, Henning S, Katiyar V, Adhikari R (2019) Compostable composites of wheat stalk micro-and nanocrystalline cellulose and poly(butylene adipate-co-terephthalate): surface properties and degradation behavior. J Appl Polym Sci 136(43):48149. https://doi.org/10.1002/app.48149
113. Ahankari SS, Subhedar AR, Bhadauria SS, Dufresne A (2021) Nanocellulose in food packaging: A review. Carbohydr Polym 255:117479. https://doi.org/10.1016/j.carbpol.2020.117479
114. Wang J, Han X, Zhang C, Liu K, Duan G (2022) Source of nanocellulose and its application in nanocomposite packaging material: a review. Nanomaterials 12(18):3158. https://doi.org/10.3390/nano12183158
115. Jenol MA, Norrrahim MNF, Nurazzi NM (2022) Nanocellulose nanocomposites in textiles. in industrial applications of

nanocellulose and Its nanocomposites. Elsevier, Netherlands, pp 397–408
116. Reshmy R, Thomas D, Philip E, Paul SA, Madhavan A, Sindhu R, Binod P, Pugazhendhi A, Sirohi R, Tarafdar A, Pandey A (2021) Potential of nanocellulose for wastewater treatment. Chemosphere 281:130738. https://doi.org/10.1016/j.chemosphere.2021.130738
117. Guo A, Sun Z, Sathitsuksanoh N, Feng H (2020) A review on the application of nanocellulose in cementitious materials. Nanomaterials 10(12):2476. https://doi.org/10.3390/nano10122476
118. Lasrado D, Ahankari S, Kar K (2020) Nanocellulose-based polymer composites for energy applications—a review. J Appl Polym Sci 137(27):48959. https://doi.org/10.1002/app.48959
119. Subhedar A, Bhadauria S, Ahankari S, Kargarzadeh H (2021) Nanocellulose in biomedical and biosensing applications: a review. Int J Biol Macromol 166:587–600. https://doi.org/10.1016/j.ijbiomac.2020.10.217
120. Chakrabarty A, Teramoto Y (2018) Recent advances in nanocellulose composites with polymers: a guide for choosing partners and how to incorporate them. Polymers 10(5):517. https://doi.org/10.3390/polym10050517
121. Ferreira FV, Dufresne A, Pinheiro IF, Souza DHS, Gouveia RF, Mei LHI, Lona LMF (2018) How do cellulose nanocrystals affect the overall properties of biodegradable polymer nanocomposites: a comprehensive review. Eur Polymer J 108:274–285. https://doi.org/10.1016/j.eurpolymj.2018.08.045
122. Zinge C, Kandasubramanian B (2020) Nanocellulose based biodegradable polymers. Eur Polym J 133:109758. https://doi.org/10.1016/j.eurpolymj.2020.109758
123. Sucinda EF, Abdul Majid MS, Ridzuan MJM, Cheng EM, Alshahrani HA, Mamat N (2021) Development and characterisation of packaging film from Napier cellulose nanowhisker reinforced polylactic acid (PLA) bionanocomposites. Int J Biol Macromol 187:43–53. https://doi.org/10.1016/j.ijbiomac.2021.07.069
124. Niu X, Huan S, Li H, Pan H, Rojas OJ (2021) Transparent films by ionic liquid welding of cellulose nanofibers and polylactide: enhanced biodegradability in marine environments. J Hazard Mater 402:124073. https://doi.org/10.1016/j.jhazmat.2020.124073
125. Asraf NH, Adli SA, Barre MS, Ali FB, Anuar H (2019) Degradation properties of biodegradable polymers. J Wastes Biomass Manag 1(2):05–08. https://doi.org/10.26480/jwbm.02.2019.05.08
126. Faraj H, Sollogoub C, Guinault A, Gervais M, Bras J, Salmi-Mani H, Roger P, le Gars M, Domenek S (2021) A comparative study of the thermo-mechanical properties of polylactide/cellulose nanocrystal nanocomposites obtained by two surface compatibilization strategies. Mater Today Commun 29:102907. https://doi.org/10.1016/j.mtcomm.2021.102907
127. Mujica-Garcia A, Hooshmand S, Skrifvars M, Kenny JM, Oksman K, Peponi L (2016) Poly(lactic acid) melt-spun fibers reinforced with functionalized cellulose nanocrystals. RSC Adv 6(11):9221–9231. https://doi.org/10.1039/C5RA22818B
128. Zaaba NF, Jaafar M, Ismail H (2021) Tensile and morphological properties of nanocrystalline cellulose and nanofibrillated cellulose reinforced <scp>PLA</scp> bionanocomposites: a review. Polym Eng Sci 61(1):22–38. https://doi.org/10.1002/pen.25560
129. Bagheriasl D, Safdari F, Carreau PJ, Dubois C, Riedl B (2019) Development of cellulose nanocrystal-reinforced polylactide: a comparative study on different preparation methods. Polym Compos 40(S1):101–113. https://doi.org/10.1002/pc.24676
130. Arslan D, Vatansever E, Sarul DS, Kahraman Y, Gunes G, Durmus A, Nofar M (2020) Effect of preparation method on the properties of polylactide/cellulose nanocrystal nanocomposites. Polym Compos 41(10):4170–4180. https://doi.org/10.1002/pc.25701
131. Wang YY, Yu H-Y, Yang L, Abdalkarim SYH, Chen W-L (2019) Enhancing long-term biodegradability and UV-shielding performances of transparent polylactic acid nanocomposite films by adding cellulose nanocrystal-zinc oxide hybrids. Int J Biol Macromol 141:893–905. https://doi.org/10.1016/j.ijbiomac.2019.09.062
132. Bauli CR, Rocha DB, RosaDos DS (2019) Composite films of ecofriendly lignocellulosic nanostructures in biodegradable polymeric matrix. SN Appl Sci 1(7):774. https://doi.org/10.1007/s42452-019-0765-0
133. Morelli CL, Belgacem N, Bretas RES, Bras J (2016) Melt extruded nanocomposites of polybutylene adipate-co-terephthalate (PBAT) with phenylbutyl isocyanate modified cellulose nanocrystals. J Appl Polym Sci 133(34):1–9. https://doi.org/10.1002/app.43678
134. Vatansever E, Arslan D, Sarul DS, Kahraman Y, Gunes G, Durmus A, Nofar M (2020) Development of CNC-reinforced PBAT nanocomposites with reduced percolation threshold: a comparative study on the preparation method. J Mater Sci 55(32):15523–15537. https://doi.org/10.1007/s10853-020-05105-4
135. Zhang X, Ma P, Zhang Y (2016) Structure and properties of surface-acetylated cellulose nanocrystal/poly(butylene adipate-co-terephthalate) composites. Polym Bull 73(7):2073–2085. https://doi.org/10.1007/s00289-015-1594-y
136. Hosseinnezhad R, Vozniak I, Zaïri F (2021) In situ generation of green hybrid nanofibrillar polymer-polymer composites—a novel approach to the triple shape memory polymer formation. Polymers 13(12):1900. https://doi.org/10.3390/polym13121900
137. Burillo G, Clough RL, Czvikovszky T, Guven O, le Moel A, Liu W, Singh A, Yang J, Zaharescu T (2002) Polymer recycling: potential application of radiation technology. Radiat Phys Chem 64(1):41–51. https://doi.org/10.1016/S0969-806X(01)00443-1
138. Güven, O., & Zengin, F. (2011). Preparation of Polypropylene/Montmorillonite Nanocomposites Using Ionizing Radiation. *Report of the 1st RCM on Radiation Curing of Composites for Enhancing the Features and Utility in Health Care and Industry. Working Material*, *July*, 145–156. http://www-naweb.iaea.org/napc/iachem/working_materials/RC-1207-1-report.pdf
139. Andrade MS, Ishikawa OH, Costa RS, Seixas MVS, Rodrigues RCLB, Moura EAB (2022) Development of sustainable food packaging material based on biodegradable polymer reinforced with cellulose nanocrystals. Food Packag Shelf Life 31:100807. https://doi.org/10.1016/j.fpsl.2021.100807
140. Tayeb A, Amini E, Ghasemi S, Tajvidi M (2018) Cellulose nanomaterials—binding properties and applications: a review. Molecules 23(10):2684. https://doi.org/10.3390/molecules23102684
141. Behera K, Chang Y-H, Chiu F-C (2021) Manufacturing poly(butylene adipate-co-terephthalate)/high density polyethylene blend-based nanocomposites with enhanced burning anti-dripping and physical properties—effects of carbon nanofillers addition. Compos Part B: Eng 217:108878. https://doi.org/10.1016/j.compositesb.2021.108878
142. Farah S, Anderson DG, Langer R (2016) Physical and mechanical properties of PLA, and their functions in widespread applications—a comprehensive review. Adv Drug Deliv Rev 107:367–392. https://doi.org/10.1016/j.addr.2016.06.012
143. Li M, Jia Y, Shen X, Shen T, Tan Z, Zhuang W, Zhao G, Zhu C, Ying H (2021) Investigation into lignin modified PBAT/thermoplastic starch composites: Thermal, mechanical, rheological and water absorption properties. Ind Crops Prod 171(30):113916. https://doi.org/10.1016/j.indcrop.2021.113916
144. Horvath T, Kalman M, Szabo T, Roman K, Zsoldos G, Szabone Kollar M (2018) The mechanical properties of polyethylene-terephthalate (PET) and polylactic-acid (PDLLA and PLLA),

the influence of material structure on forming. IOP Conf Series: Mater Sci Eng 426(1):012018. https://doi.org/10.1088/1757-899X/426/1/012018
145. Tang D, Zhang C, Weng Y (2021) Effect of multi-functional epoxy chain extender on the weathering resistance performance of poly(butylene adipate-co-terephthalate) (PBAT). Polym Test 99:107204. https://doi.org/10.1016/j.polymertesting.2021.107204
146. Yu W, Wang X, Ferraris E, Zhang J (2019) Melt crystallization of PLA/Talc in fused filament fabrication. Mater Des 182:108013. https://doi.org/10.1016/j.matdes.2019.108013
147. Mohanty S, Nayak SK (2009) Starch based biodegradable PBAT nanocomposites: Effect of starch modification on mechanical, thermal, morphological and biodegradability behavior. Int J Plast Technol 13(2):163–185. https://doi.org/10.1007/s12588-009-0013-3
148. Mohanty S, Nayak SK (2010) Biodegradable nanocomposites of poly (butylene adipate-co-terephthalate) (PBAT) with organically modified nanoclays. Int J Plast Technol 14(2):192–212. https://doi.org/10.1007/s12588-010-0018-y
149. Chinh NT, Hoang T (2022) Review polylactic acid : synthesis, properties and technical and biomedical applications. Vietnam J Sci Technol 60(3):283–313. https://doi.org/10.15625/2525-2518/16721
150. Tábi T, Ageyeva T, Kovács JG (2021) Improving the ductility and heat deflection temperature of injection molded poly(lactic acid) products: a comprehensive review. Polym Test 101:107282. https://doi.org/10.1016/j.polymertesting.2021.107282
151. Luo Y, Lin Z, Guo G (2019) biodegradation assessment of poly (lactic acid) filled with functionalized Titania nanoparticles (PLA/TiO2) under compost conditions. Nanoscale Res Lett 14(1):56. https://doi.org/10.1186/s11671-019-2891-4
152. Boonmee J, Kositanont C, Leejarkpai T (2016) Biodegradation of poly(lactic acid), poly(hydroxybutyrate-co-hydroxyvalerate), poly(butylene succinate) and poly(butylene adipate-co-terephthalate) under anaerobic and oxygen limited thermophilic conditions. EnvironmentAsia 9(1):107–115. https://doi.org/10.14456/ea.1473.13
153. Boonmee C, Kositanont C, Leejarkpai T (2016) Degradation of poly (lactic acid) under simulated landfill conditions. Environ Nat Res J 14(2):1–9. https://doi.org/10.14456/ennrj.2016.8
154. Jandas PJ, Mohanty S, Nayak SK (2013) Sustainability, compostability, and specific microbial activity on agricultural mulch films prepared from poly(lactic acid). Ind Eng Chem Res 52(50):17714–17724. https://doi.org/10.1021/ie4023429
155. Kalita NK, Bhasney SM, Kalamdhad A, Katiyar V (2020) Biodegradable kinetics and behavior of bio-based polyblends under simulated aerobic composting conditions. J Environ Manag 261:110211. https://doi.org/10.1016/j.jenvman.2020.110211
156. Mbarki K, Fersi M, Louati I, Elleuch B, Sayari A (2021) Biodegradation study of PDLA/cellulose microfibres biocomposites by *Pseudomonas aeruginosa*. Environ Technol 42(5):731–742. https://doi.org/10.1080/09593330.2019.1643926
157. Castro-Aguirre E, Auras R, Selke S, Rubino M, Marsh T (2018) Enhancing the biodegradation rate of poly(lactic acid) films and PLA bio-nanocomposites in simulated composting through bioaugmentation. Polym Degrad Stab 154:46–54. https://doi.org/10.1016/j.polymdegradstab.2018.05.017
158. Sedničková M, Pekařová S, Kucharczyk P, Bočkaj J, Janigová I, Kleinová A, Jochec-Mošková D, Omaníková L, Perďochová D, Koutný M, Sedlařík V, Alexy P, Chodák I (2018) Changes of physical properties of PLA-based blends during early stage of biodegradation in compost. Int J Biol Macromol 113:434–442. https://doi.org/10.1016/j.ijbiomac.2018.02.078
159. Anunciado MB, Hayes DG, Astner AF, Wadsworth LC, Cowan-Banker CD, Gonzalez JELY, DeBruyn JM (2021) Effect of environmental weathering on biodegradation of biodegradable plastic mulch films under ambient soil and composting conditions. J Polym Environ 29(9):2916–2931. https://doi.org/10.1007/s10924-021-02088-4
160. Ruggero F, Onderwater RCA, Carretti E, Roosa S, Benali S, Raquez J-M, Gori R, Lubello C, Wattiez R (2021) Degradation of film and rigid bioplastics during the thermophilic phase and the maturation phase of simulated composting. J Polym Environ 29(9):3015–3028. https://doi.org/10.1007/s10924-021-02098-2
161. Sintim HY, Bary AI, Hayes DG, English ME, Schaeffer SM, Miles CA, Zelenyuk A, Suski K, Flury M (2019) Release of micro- and nanoparticles from biodegradable plastic during in situ composting. Sci Total Environ 675:686–693. https://doi.org/10.1016/j.scitotenv.2019.04.179
162. Panyachanakul T, Sorachart B, Lumyong S, Lorliam W, Kitpreechavanich V, Krajangsang S (2019) Development of biodegradation process for Poly(DL-lactic acid) degradation by crude enzyme produced by actinomadura keratinilytica strain T16–1. Electron J Biotechnol 40:52–57. https://doi.org/10.1016/j.ejbt.2019.04.005
163. Decorosi F, Exana ML, Pini F, Adessi A, Messini A, Giovannetti L, Viti C (2019) The Degradative capabilities of new amycolatopsis isolates on polylactic acid. Microorganisms 7(12):590. https://doi.org/10.3390/microorganisms7120590
164. Sriyapai P, Chansiri K, Sriyapai T (2018) Isolation and characterization of polyester-based plastics-degrading bacteria from compost soils. Microbiology 87(2):290–300. https://doi.org/10.1134/S0026261718020157
165. Müller CA, Perz V, Provasnek C, Quartinello F, Guebitz GM, Berg G (2017) Discovery of polyesterases from moss-associated microorganisms. Appl Environ Microbiol 83(4):1–13. https://doi.org/10.1128/AEM.02641-16
166. Miksch L, Gutow L, Saborowski R (2021) pH-stat titration: a rapid assay for enzymatic degradability of bio-based polymers. Polymers 13(6):860. https://doi.org/10.3390/polym13060860
167. Muroi F, Tachibana Y, Soulenthone P, Yamamoto K, Mizuno T, Sakurai T, Kobayashi Y, Kasuya K (2017) Characterization of a poly(butylene adipate- co -terephthalate) hydrolase from the aerobic mesophilic bacterium *Bacillus pumilus*. Polym Degrad Stab 137:11–22. https://doi.org/10.1016/j.polymdegradstab.2017.01.006
168. Satti SM, Shah AA, Auras R, Marsh TL (2017) Isolation and characterization of bacteria capable of degrading poly(lactic acid) at ambient temperature. Polym Degrad Stab 144:392–400. https://doi.org/10.1016/j.polymdegradstab.2017.08.023
169. Bubpachat T, Sombatsompop N, Prapagdee B (2018) Isolation and role of polylactic acid-degrading bacteria on degrading enzymes productions and PLA biodegradability at mesophilic conditions. Polym Degrad Stab 152:75–85. https://doi.org/10.1016/j.polymdegradstab.2018.03.023
170. Wallace PW, Haernvall K, Ribitsch D, Zitzenbacher S, Schittmayer M, Steinkellner G, Gruber K, Guebitz GM, Birner-Gruenberger R (2017) PpEst is a novel PBAT degrading polyesterase identified by proteomic screening of Pseudomonas pseudoalcaligenes. Appl Microbiol Biotechnol 101(6):2291–2303. https://doi.org/10.1007/s00253-016-7992-8
171. Karimi-Avargani M, Bazooyar F, Biria D, Zamani A, Skrifvars M (2020) The special effect of the Aspergillus flavus and its enzymes on biological degradation of the intact polylactic acid (PLA) and PLA-Jute composite. Polym Degrad Stab 179:109295. https://doi.org/10.1016/j.polymdegradstab.2020.109295
172. Hegyesi N, Zhang Y, Kohári A, Polyák P, Sui X, Pukánszky B (2019) Enzymatic degradation of PLA/cellulose nanocrystal

composites. Ind Crops Prod 141:111799. https://doi.org/10.1016/j.indcrop.2019.111799
173. Aarthy M, Puhazhselvan P, Aparna R, George AS, Gowthaman MK, Ayyadurai N, Masaki K, Nakajima-Kambe T, Kamini NR (2018) Growth associated degradation of aliphatic-aromatic copolyesters by Cryptococcus sp. MTCC 5455. Polym Degrad Stab 152:20–28. https://doi.org/10.1016/j.polymdegradstab.2018.03.021
174. Tesei D, Quartinello F, Guebitz GM, Ribitsch D, Nöbauer K, Razzazi-Fazeli E, Sterflinger K (2020) Shotgun proteomics reveals putative polyesterases in the secretome of the rock-inhabiting fungus *Knufia chersonesos*. Sci Rep 10(1):9770. https://doi.org/10.1038/s41598-020-66256-7
175. Farias da Silva JM, Soares BG (2021) Epoxidized cardanol-based prepolymer as promising biobased compatibilizing agent for PLA/PBAT blends. Polym Testing 93:106889. https://doi.org/10.1016/j.polymertesting.2020.106889
176. Phetwarotai W, Phusunti N, Aht-Ong D (2019) Preparation and characteristics of poly(butylene adipate-co-terephthalate)/polylactide blend films via synergistic efficiency of plasticization and compatibilization. Chin J Polym Sci 37(1):68–78. https://doi.org/10.1007/s10118-019-2174-7
177. Kumar A, Tumu VR, Ray Chowdhury S, SVS RR (2019) A green physical approach to compatibilize a bio-based poly (lactic acid)/lignin blend for better mechanical, thermal and degradation properties. Int J Biol Macromol 121:588–600. https://doi.org/10.1016/j.ijbiomac.2018.10.057
178. Ahmed J, Mushtaq S, Adeel M (2021) Fabrication of ethylene-vinyl acetate copolymer/polyamide/modified sepiolite composite with improved physical properties via e-beam irradiation. Radiat Phys Chem 189:109779. https://doi.org/10.1016/j.radphyschem.2021.109779
179. Kumar A, Tumu VR (2019) Physicochemical properties of the electron beam irradiated bamboo powder and its bio-composites with PLA. Compos Part B: Eng 175(July):107098. https://doi.org/10.1016/j.compositesb.2019.107098
180. Entezam M, Aghjeh MKR, Ghaffari M (2017) Electron beam irradiation induced compatibilization of immiscible polyethylene/ethylene vinyl acetate (PE/EVA) blends: Mechanical properties and morphology stability. Radiat Phys Chem 131:22–27. https://doi.org/10.1016/j.radphyschem.2016.10.016
181. Xia X, Shi X, Liu W, He S, Zhu C, Liu H (2020) Effects of gamma irradiation on properties of PLA/flax composites. Iran Polym J 29(7):581–590. https://doi.org/10.1007/s13726-020-00820-w
182. Malinowski R, Moraczewski K, Raszkowska-Kaczor A (2020) Studies on the uncrosslinked fraction of PLA/PBAT blends modified by electron radiation. Materials 13(5):1068. https://doi.org/10.3390/ma13051068
183. Iuliano A, Fabiszewska A, Kozik K, Rzepna M, Ostrowska J, Dębowski M, Plichta A (2021) Effect of electron-beam radiation and other sterilization techniques on structural, mechanical and microbiological properties of thermoplastic starch blend. J Polym Environ 29(5):1489–1504. https://doi.org/10.1007/s10924-020-01972-9
184. Jeon JS, Han DH, Shin BY (2018) Improvements in the rheological properties, impact strength, and the biodegradability of pla/pcl blend compatibilized by electron-beam irradiation in the presence of a reactive agent. Adv Mater Sci Eng 2018:1–8. https://doi.org/10.1155/2018/5316175
185. Kumar A, Venkatappa Rao T, Ray Chowdhury S, Ramana Reddy SVS (2018) Optimization of mechanical, thermal and hydrolytic degradation properties of Poly (lactic acid)/Poly (ethylene-co-glycidyl methacrylate)/Hexagonal boron nitride blend-composites through electron-beam irradiation. Nucl Instrum Methods Phys Res, Sect B 428:38–46. https://doi.org/10.1016/j.nimb.2018.05.011
186. Zembouai I, Kaci M, Bruzaud S, Dumazert L, Bourmaud A, Mahlous M, Lopez-Cuesta JM, Grohens Y (2016) Gamma irradiation effects on morphology and properties of PHBV/PLA blends in presence of compatibilizer and cloisite 30B. Polym Test 49:29–37. https://doi.org/10.1016/j.polymertesting.2015.11.003
187. de Castro DP, Sartori MDN, de Silva LG, A. e. (2019) Effects of gamma radiation on the properties of the thermoplastic starch/poly (Butylene Adipate-co-Terephthalate) blends. Mater Res 22(1):1–6. https://doi.org/10.1590/1980-5373-mr-2019-0072
188. Huerta-Cardoso O, Durazo-Cardenas I, Longhurst P, Simms NJ, Encinas-Oropesa A (2020) Fabrication of agave tequilana bagasse/PLA composite and preliminary mechanical properties assessment. Ind Crops Prod 152:112523. https://doi.org/10.1016/j.indcrop.2020.112523
189. Chaitanya S, Singh I (2018) Ecofriendly treatment of aloe vera fibers for PLA based green composites. Int J Precis Eng Manuf-Green Technol 5(1):143–150. https://doi.org/10.1007/s40684-018-0015-8
190. Hong H, Xiao R, Guo Q, Liu H, Zhang H (2019) Quantitively characterizing the chemical composition of tailored bagasse fiber and its effect on the thermal and mechanical properties of polylactic acid-based composites. Polymers 11(10):1567. https://doi.org/10.3390/polym11101567
191. Manral A, Ahmad F, Chaudhary V (2020) Static and dynamic mechanical properties of PLA bio-composite with hybrid reinforcement of flax and jute. Mater Today: Proc 25:577–580. https://doi.org/10.1016/j.matpr.2019.07.240
192. Siva R, Nemali SSR, Kunchapu SK, Gokul K, Kumar AT (2021) Comparison of Mechanical properties and water absorption test on injection molding and extrusion—injection molding thermoplastic hemp fiber composite. Mater Today: Proc 47:4382–4386. https://doi.org/10.1016/j.matpr.2021.05.189
193. Jamadi AH, Razali N, Petrů M, Taha MM, Muhammad N, Ilyas RA (2021) Effect of chemically treated kenaf fibre on mechanical and thermal properties of pla composites prepared through fused deposition modeling (FDM). Polymers 13(19):3299. https://doi.org/10.3390/polym13193299
194. Yu T, Li Y (2014) Influence of poly(butylenes adipate-co-terephthalate) on the properties of the biodegradable composites based on ramie/poly(lactic acid). Compos A Appl Sci Manuf 58:24–29. https://doi.org/10.1016/j.compositesa.2013.11.013
195. Gupta M, Singh R (2019) PLA-coated sisal fibre-reinforced polyester composite: water absorption, static and dynamic mechanical properties. J Compos Mater 53(1):65–72. https://doi.org/10.1177/0021998318780227
196. Liu Z, Lei Q, Xing S (2019) Mechanical characteristics of wood, ceramic, metal and carbon fiber-based PLA composites fabricated by FDM. J Market Res 8(5):3741–3751. https://doi.org/10.1016/j.jmrt.2019.06.034
197. Xie X, Zhang C, Weng Y, Diao X, Song X (2020) Effect of diisocyanates as compatibilizer on the properties of BF/PBAT composites by in situ reactive compatibilization. Crosslink Chain Ext Mater 13(3):806. https://doi.org/10.3390/ma13030806
198. Marques MFV, Lunz JN, Aguiar VO, Grafova I, Kemell M, Visentin F, Sartori A, Grafov A (2015) Thermal and mechanical properties of sustainable composites reinforced with natural fibers. J Polym Environ 23(2):251–260. https://doi.org/10.1007/s10924-014-0687-2
199. Siyamak S, Ibrahim NA, Abdolmohammadi S, Yunus WMZW, Rahman MZAB (2012) Effect of fiber esterification on fundamental properties of oil palm empty fruit bunch fiber/

poly(butylene adipate-co-terephthalate) biocomposites. Int J Mol Sci 13(2):1327–1346. https://doi.org/10.3390/ijms13021327
200. Phongam N, Dangtungee R, Siengchin S (2015) Comparative studies on the mechanical properties of nonwoven- and woven-flax-fiber-reinforced poly(butylene adipate-co-terephthalate)-based composite laminates. Mech Compos Mater 51(1):17–24. https://doi.org/10.1007/s11029-015-9472-0
201. Conzatti L, Brunengo E, Utzeri R, Castellano M, Hodge P, Stagnaro P (2018) Macrocyclic oligomers as compatibilizing agent for hemp fibres/biodegradable polyester eco-composites. Polymer 146:396–406. https://doi.org/10.1016/j.polymer.2018.05.053
202. Andrzejewski J, Grad K, Wiśniewski W, Szulc J (2021) The use of agricultural waste in the modification of poly(lactic acid)-based composites intended for 3D printing applications. the use of toughened blend systems to improve mechanical properties. J Compos Sci 5(10):253. https://doi.org/10.3390/jcs5100253
203. Feng J, Zhang W, Wang L, He C (2020) Performance comparison of four kinds of straw/PLA/PBAT wood plastic composites. BioResources 15(2):2596–2604. https://doi.org/10.15376/biores.15.2.2596-2604
204. Andrzejewski J, Nowakowski M (2021) Development of toughened flax fiber reinforced composites. modification of poly(lactic acid)/poly(butylene adipate-co-terephthalate) blends by reactive extrusion process. Materials 14(6):1523. https://doi.org/10.3390/ma14061523
205. Xiao X, Chevali VS, Song P, He D, Wang H (2019) Polylactide/hemp hurd biocomposites as sustainable 3D printing feedstock. Compos Sci Technol 184:107887. https://doi.org/10.1016/j.compscitech.2019.107887
206. Sis ALM, Ibrahim NA, Yunus WMZW (2013) Effect of (3-aminopropyl)trimethoxysilane on mechanical properties of PLA/PBAT blend reinforced kenaf fiber. Iran Polym J 22(2):101–108. https://doi.org/10.1007/s13726-012-0108-0
207. Wu H, Hao M (2019) Strengthening and toughening of polylactide/sisal fiber biocomposites via in-situ reaction with epoxy-functionalized oligomer and poly (butylene-adipate-terephthalate). Polymers 11(11):1747. https://doi.org/10.3390/polym11111747
208. Chaiwutthinan P, Chuayjuljit S, Srasomsub S, Boonmahitthisud A (2019) Composites of poly(lactic acid)/poly(butylene adipate–co–terephthalate) blend with wood fiber and wollastonite: physical properties, morphology, and biodegradability. J Appl Polym Sci 136(21):47543. https://doi.org/10.1002/app.47543
209. Dou Q, Cai J (2016) Investigation on polylactide (PLA)/Poly(butylene adipate-co-terephthalate) (PBAT)/Bark flour of plane tree (PF) eco-composites. Materials 9(5):393. https://doi.org/10.3390/ma9050393
210. Pracella M, Haque M-U, Puglia D (2014) Morphology and properties tuning of PLA/cellulose nanocrystals bio-nanocomposites by means of reactive functionalization and blending with PVAc. Polymer 55(16):3720–3728. https://doi.org/10.1016/j.polymer.2014.06.071
211. Sung SH, Chang Y, Han J (2017) Development of polylactic acid nanocomposite films reinforced with cellulose nanocrystals derived from coffee silverskin. Carbohyd Polym 169:495–503. https://doi.org/10.1016/j.carbpol.2017.04.037
212. Mármol G, Gauss C, Fangueiro R (2020) Potential of cellulose microfibers for PHA and PLA biopolymers reinforcement. Molecules 25(20):4653. https://doi.org/10.3390/molecules25204653
213. López de Dicastillo C, Garrido L, Alvarado N, Romero J, Palma J, Galotto M (2017) Improvement of polylactide properties through cellulose nanocrystals embedded in poly(vinyl alcohol) electrospun nanofibers. Nanomaterials 7(5):106. https://doi.org/10.3390/nano7050106